Numerical Modelling of Non-Load Bearing LSF Walls under Fire Conditions

Poologanathan Keerthan and Mahen Mahendran

Faculty of Built Environment and Engineering

Queensland University of Technology, Brisbane, QLD 4000, Australia

Abstract: Recently an innovative composite panel system was developed, where a thin insulation layer was used externally between two plasterboards to improve the fire performance of light gauge cold-formed steel frame (LSF) walls. In this research, finite element thermal models of both the traditional LSF wall panels with cavity insulation and the new LSF composite wall panels were developed to simulate their thermal behaviour under standard and realistic fire conditions. Suitable apparent thermal properties of gypsum plasterboard, insulation materials and steel were proposed and used. The developed models were then validated by comparing their results with available fire test results. This paper presents the details of the developed finite element models of small scale non-load bearing LSF wall panels and the thermal analysis results. It has shown that accurate finite element models can be used to simulate the thermal behaviour of small scale LSF walls with varying configurations of insulations and plasterboards. The numerical results show that the use of cavity insulation was detrimental to the fire rating of LSF walls while the use of external insulation offered superior thermal protection to them. Effects of real fire conditions are also presented.

Keywords: *Non-Load Bearing LSF Walls, Finite Element Analysis, Gypsum Plasterboard, Insulation, Cold-formed Steel Studs, Thermal Performance, Standard Fire, Real Fire.*

Corresponding author's email address: m.mahendran@qut.edu.au

1. Introduction

In recent times, LSF wall and floor systems are increasingly used in low-rise and multi-storey buildings, but without a full understanding of their fire performance. Figure 1 shows the use of gypsum plasterboards in the Light Gauge Steel Framing (LSF) wall systems. Currently LSF wall and floor systems are made of cold-formed thin-walled steel lipped channel sections and gypsum plasterboards. Under fire conditions, cold-formed thin-walled steel stud and joist sections heat up quickly resulting in fast reduction in their strength and stiffness. Therefore they are commonly used in structural wall and floor systems with plasterboard linings on both sides used as fire protection (Figure 1). Gypsum plasterboard protects steel studs and joists during building fires by delaying the temperature rise.

Cavity insulated LSF walls are often used for the purpose of climate control (in exterior walls) and acoustic benefits. However, they are also required to be fire rated. Hence many researchers investigated the fire ratings of LSF wall systems with different types of insulations in the wall cavities. Sultan [1] performed full scale fire resistance tests on non-load bearing gypsum board wall assemblies and noted that when rockwool was used as cavity insulation the fire resistance rating increased by 54% over the non-insulated wall assemblies while glass fibre did not affect the fire performance. Sultan [1] found that cellulose fibre cavity insulation reduced the fire resistance rating. Kodur and Sultan [2] conducted 14 full-scale fire resistance tests of load bearing LSF wall panels. They found that the insulation type, number of gypsum board layers and stud-spacing have a significant influence on the fire resistance of steel wall assemblies. They showed that LSF wall assemblies without insulation provided higher fire resistance than cavity insulated LSF wall assemblies. The stud walls with wider stud spacing had higher fire resistance than the narrow spaced walls. Feng et al. [3] conducted eight small-scale fire tests of non-load bearing wall panels to investigate the thermal performance of thin steel channel sections under standard fire conditions. The tests consisted of 300x300 mm LSF panels with different types of steel section, number of gypsum boards with or without cavity insulation. Feng et al. [3] found that the thermal performance of cold-formed thin-walled steel channel wall panels was not affected by the type of insulation and that the thermal performance of wall panels improved with the use of cavity insulation.

In summary, past research has provided varying results about the benefits of cavity insulation to the fire rating of LSF wall systems. Extensive research has been undertaken on the fire

performance of LSF walls with various configurations in the USA and Canada. However, only limited research has been undertaken on the fire performance of LSF wall systems used in Australia. Australian building industry opinion is that new LSF wall systems with increased fire rating are needed. Hence Kolarkar and Mahendran [4] developed a new composite LSF wall panel system in which a thin insulation layer was used externally between plasterboards instead of the conventional cavity insulation located within the stud space. Since the new composite LSF wall panels have an external insulation layer between the plasterboards, they also provide climate control and acoustic benefits. However, it leads to slightly increased wall thickness.

Figure 2(a) shows the innovative composite panel while Figure 2(b) shows their LSF wall system. Kolarkar and Mahendran [4] found that composite LSF wall panels provided a better quality thermal envelope than the cavity insulated LSF wall panels. Kolarkar [5] conducted a series of fire tests to investigate the thermal performance of non-load bearing LSF wall panels made of the new composite panels under standard fire conditions. However, numerical studies on the thermal performance of these non-load bearing LSF wall panels have not been conducted. Hence numerical analyses were performed to investigate the thermal performance of the innovative non-load bearing LSF wall panels under standard and realistic fire conditions. These numerical analyses also included the traditional LSF wall systems with and without cavity insulation to investigate the differences in their thermal performances. This numerical study was part of a large research project on the structural and thermal performance of LSF wall panels made of Australian high strength steels and plasterboards undertaken at the Queensland University of Technology. This paper presents the details of the numerical study of the thermal performance of innovative non-load bearing LSF wall panels under fire conditions. It includes the details of finite element models of non-load bearing LSF wall panels, the thermal analysis results under standard and real fire conditions, and their comparisons with experimental results. It also includes a brief literature review of the thermal properties of gypsum plasterboard, insulation materials and steel.

2. Thermal Properties of Gypsum Plasterboard, Insulation Materials and Steel

2.1. Gypsum Plasterboard

In order to develop suitable finite element models of Australian gypsum plasterboard [6], thermal properties of gypsum plasterboard were summarized based on a series of

experimental results [6] and past research work [7-9]. This was achieved by developing suitable thermal property values based on a comparison of all the results, followed by a series of thermal analyses of plasterboards and plasterboard assemblies using SAFIR and the proposed thermal properties. Suitable adjustments were then made to the thermal properties until a good agreement was obtained between the time-temperature profile results of numerical analyses and those obtained from Kolarkar's [5] fire tests of plasterboards. Figure 3(a) shows the proposed thermal conductivity of gypsum plasterboard. The proposed apparent thermal conductivity of plasterboard was based on small scale plasterboard fire tests during which the fire side temperature of plasterboard went up to 1180^{o}C. The plasterboard fall-off in these tests was expected to occur at about 1200^{o}C. In order to simulate the effect of plasterboard fall off, a rapid rise in the curve was proposed at 1200^{o}C as shown in Figure 3a.

Past research showed some discrepancy in relation to the second dehydration reaction. However, it is concluded that the first and second dehydrations occur at 100 to 150ºC and 150 to 200ºC, respectively, based on our experiments [6]. Decomposition of Calcium Carbonate occurs at 670ºC, which is similar to Sultan's [1] and Wakili et al.'s [10] values. These outcomes including the third peak to simulate the effect of decomposition of Calcium Carbonate were used in the proposed specific heat versus temperature curves. At about 400ºC, an exothermic reaction occurs, in which the molecular structure of the soluble crystal restructures itself into a lower insoluble energy state (Figure 3b). This observation is simliar to Manzello et al.'s [11] findings. In order to propose suitable specific heat values, a similar approach was used as for thermal conductivity. When the lower bound experimental results of specific heat were used as input to SAFIR [7], the time-temperature profiles agreed well with experimental results of plasterboards from Kolarkar [5]. Figure 3(b) also shows the proposed specific heat values as a function of temperature and compares them with test and past researcher's specific heat values [1,9,12] while Figure 3(c) shows the relative density values as a function of temperature and compares them with those from tests and past research [9,12]. Further details of the proposed thermal properties of gypsum plasterboards are given in Keerthan and Mahendran [6].

The specific volumetric enthalpy of gypsum plasterboard is given by the area under the specific heat multiplied by the density versus temperature curve as shown in Equation (1). The proposed specific volumetric enthalpy values were used as input to SAFIR [6] in our thermal analyses.

$$E(T) = \int_{T_A}^{T} C_P(T)\rho(T)dT \quad (1)$$

where E(T) is the specific volumetric enthalpy in J/m^3 at temperature T, C_p (T) is the specific heat (J/(kg^{o}C)) at temperature T and ρ (T) is the density (kg/m^3) at temperature T, and T_A is the ambient temperature. Keerthan and Mahendran [6] recommended a convective coefficient (h) of 25 W/m^2/K for the exposed side (fire) of plasterboard and 10 W/m^2/K for its unexposed side. They recommended 0.9 as emissivity (ε) of plasterboard for both exposed and unexposed surfaces. When the recommended emissivity and convective coefficient values were used as input to SAFIR, the time-temperature profiles agreed well with Kolarkar's [5] fire test results.

2.2. Insulation Materials

The new composite LSF wall system was developed with glass fibre or rockwool or cellulose fibre insulation sandwiched between the plasterboard layers. Glass wool is formed from molten glass (silicate) fibres and is currently the most commonly used insulation in Australia, particularly in residential construction. Rockwool insulation typically provides much higher levels of insulation being formed from basalt or iron ore blast furnace slag to provide higher density. Keerthan and Mahendran [6] proposed suitable thermal properties of gypsum plasterboard for use in their numerical analyses (Section 2.1). These apparent thermal properties were initially based on the results from a series of tests and past research work, and then revised to provide a good correlation of numerical results with plasterboard experimental results in Kolarkar [5]. A similar procedure was used in the case of insulations.

In order to develop suitable finite element models of composite panels [13], thermal properties of insulation were summarized based on our experimental results and past research work [14-16]. This was achieved by developing suitable thermal property values based on a comparison of all the results, followed by a series of thermal analyses of composite panels and composite panel assemblies using SAFIR and these proposed thermal properties. Suitable adjustments were then made to the thermal properties of insulation materials until a good agreement was obtained between the time-temperature profile results of numerical analyses and those obtained from Kolarkar's [5] fire tests. Table 1 presents the proposed specific heat values of rockwool, glass fibre and cellulose fibre while Figure 4 shows their proposed

thermal conductivities. When the proposed thermal conductivity and specific heat values of rockwool, glass fibre and cellulose fibre were used as input to the numerical models based on SAFIR [7], the time-temperature profiles agreed well with fire test results from Kolarkar [5]. Further details of the proposed thermal properties of insulation materials and the specific heat test procedure of plasterboard and insulation are reported in Keerthan and Mahendran [13]. Glass fibre and cellulose fibre have very low specific heat (900 and 1250 J/(kg°C) in comparison to that of gypsum plasterboard (17,500 J/(kg°C). Experimental results also showed that the specific heat of glass fibre did not change much in the temperature range of 20 to 550^{o}C. Hence the specific heats of glass fibre and cellulose fibre were considered as constants in Table 1.

Figure 4 compares the thermal conductivity values from this research with those reported by other researchers. However, the chemical composition of insulations these researchers used might have been different, which in turn could lead to differences in their thermal properties. For example, thermal properties reported by Alfawakhiri [16] are for dry-blown cellulose fibre insulation, while the cellulose fibre insulation used in this research was wet spayed.

2.3. Steel

The temperature increase of a steel member is a function of its thermal conductivity and specific heat of steel. The precision in the determination of thermal properties of steel, such as specific heat and thermal conductivity, has little influence on the thermal modelling of LSF walls under fire conditions since steel framing plays a minor role in the overall heat transfer mechanism of the LSF wall assembly [16]. The properties of steel within the SAFIR code are obtained from those given in Eurocodes [17]. The ambient density of steel is typically taken as 7850 kg/m^3 [18], which remains essentially constant with increasing temperatures.

The variation of thermal conductivity of steel with temperature is defined by Equation (2) [17]. Figure 5(a) shows the plot of thermal conductivity of steel versus temperature. For simple calculation models the thermal conductivity of steel may be considered to be independent of the steel temperature and taken as a constant value of 45 W/m/K.

$$\left.\begin{array}{l} 20^oC \le T < 800^oC \\ k = 54 - 3.33\times10^{-2}T \quad W/m/K \\ 800^oC \le T \le 1200^oC \\ k = 27.3 \;\; W/m/K \end{array}\right\} \tag{2}$$

where k and T are the thermal conductivity and temperature of steel, respectively.

The variation of specific heat of steel with temperature of steel is defined by Equation (3) [17]. Figure 5(b) shows the plot of specific heat of steel versus temperature, where the peak results from a metallurgical change at about 730°C. For simple calculation models the specific heat of steel may be considered to be independent of the steel temperature and can be taken as 600 J/(kg°C).

$$\left.\begin{array}{l} 20^oC \le T < 600^oC \\ C_p = 425 + 7.73\times10^{-1}T - 1.69\times10^{-3}T^2 + 2.22\times10^{-6}T^3 \quad J/(kg^oC) \\ 600^oC \le T < 735^oC \\ C_p = 666 + 13002/(738 - T) \quad J/(kg^oC) \\ 735^oC \le T < 900^oC \\ C_p = 545 + 17820/(T - 731) \;\; J/(kg^oC) \\ 900^oC \le T \le 1200^oC \\ C_p = 650 \quad J/(kg^oC) \end{array}\right\} \tag{3}$$

where C_p and T are the specific heat and temperature of steel, respectively.

3. Thermal Behaviour of Non-Load Bearing LSF Walls Using Experimental Studies

3.1. Test Specimens

In order to investigate the thermal performance of non-load bearing LSF wall panels, nine fire tests of small scale panels of dimensions 1280 mm x 1015 mm were conducted by

Kolarkar [5]. The wall assemblies typically consisted of three commonly used cold-formed steel lipped channel section studs (90x40x15 mm) spaced at 500 mm. The studs were fabricated from galvanized steel sheets (G500) having a nominal base metal thickness of 1.15 mm and a minimum yield strength of 500 MPa. Test specimens were built by lining the test frames with one or two layers of gypsum plasterboards manufactured by Boral Plasterboard under the product name of Firestop. All the plasterboards used were 1280 mm in width and 1015 mm in height with a thickness of 16 mm and a mass of 13 kg/m^2. There were three groups of wall specimens made of (1) no insulation (2) cavity insulation and (3) external insulation (composite panels). Three insulation materials, glass fibre, rockwool and cellulose fibre were used. Figure 6 shows the schematic diagrams of non-load bearing LSF wall test specimens used by Kolarkar [5].

In Test Specimens 7 to 9, a layer of 25 mm thick insulation was sandwiched between the two plasterboards, thus forming composite panels on either side of the steel frame. Insulation densities of Test Specimens 4, 5, 6, 7, 8 and 9 were 15.42, 100, 125, 37, 100 and 108 kg/m^3, respectively [5]. The first plasterboard layer was attached to the three studs of the steel frame by 25 mm long self-drilling bugle head screws at 300 mm centres. It included 25 mm wide plasterboard strips along its border within which the insulation layer was placed. The face plasterboard layer was then attached through the insulation layer to the base layer and the frame with 65 mm long drywall screws with bugle heads, spaced at 300 mm centres along the studs. All the connections were sufficiently rigid to resist the routine service impacts or horizontal loads. Further details of the test specimens are provided in [5].

3.2. Test Set-up

Tests were conducted using the standard fire curve given in AS 1530.4 [19], which is similar to ISO 834-1 [20] and ASTM E119 [21]. One face of the test specimens was exposed to heat in a propane-fired vertical gas furnace. Figure 7 shows the fire test set-up of non-load bearing wall panels. As shown in the figure the panels were not restrained on all four sides. Time-temperature profiles at various locations across the specimen thickness were measured during the tests using thermocouples.

3.3. Test Observations and Results

Test Specimens 1 and 2 were exposed to the standard fire curve for slightly more than three hours. At the end of the test, it was noted that both the exposed and ambient side plasterboards were severely affected. Kolarkar [5] found that the insulation failure of Specimens 1 and 2 occurred at 89 and 92 minutes, respectively. Kolarkar [5] identified that the central studs were critical in Specimens 1 and 2 as they showed higher temperatures than the end studs over the entire tests. The vertical joint is likely to reduce the fire rating of load bearing walls as the rapidly rising temperatures in the studs is likely to cause a premature structural failure of the studs.

Test Specimen 3 (No cavity insulation), Test Specimen 4 (Glass fibre as cavity insulation), Test Specimen 5 (Rockwool as cavity insulation) and Test Specimen 6 (Cellulose fibre as cavity insulation) were subjected to heat in the furnace for slightly more than three hours. Kolarkar [5] identified that Plasterboards 1 and 2 (fire side plasterboards) in Specimen 3 were about to fall off whereas they had partially fallen off in Test Specimens 4 to 6. The studs of Specimen 3 were in good condition whereas those in the cavity insulated specimens were severely damaged, in particular, Specimen 6 using cellulose fibre as cavity insulation (Figures 8(a) to (d)). The unexposed surface of all the specimens showed no signs of damage or the effect of temperature until the end. Figures 8(a) to (d) show Specimens 3 to 6 after the fire test.

The cold-formed steel frames were not twisted or bent in Test Specimens 7 to 9. The central stud was the most affected in all three specimens. The central stud in Specimen 9 (cellulose fibre as external insulation) showed the maximum damage. Figures 8(e) to (g) show Specimens 7 to 9 after the fire test. Kolarkar [5] found that LSF walls with external insulation provided a greater fire protection than those with cavity insulation.

Following conclusions were made based on fire test results [5].

- Heat transfer in the LSF wall without cavity insulation took place via conduction, convection and radiation. As a result of the faster transmission of heat mostly through radiation, the temperatures across the stud cross-sections were generally uniform, thus resulting in minimum lateral deformations (ie. reduced thermal bowing)

- Use of cavity insulation was detrimental to the fire rating of walls. It not only led to higher temperatures in the steel studs, but also to larger temperature gradients across their depth which increased thermal bowing effects.

- The heat trapped in the cavity by the insulation led to extensive stud damage in cavity insulated specimens. In comparison, non-insulated Specimen 3 steel studs were in good condition.

- Use of external insulation offered superior thermal protection to the studs resulting in a generally uniform temperature distribution across their cross-sections, thus producing minimum early lateral deformation (thermal bowing).

- The difference in temperatures of the individual studs in the externally insulated specimens was not critical as the heat radiation in an open cavity is very fast leading to a quick balance of temperatures in the studs. This would help in reducing the building up of internal stresses in the frame caused by unequal expansions of studs.

Test specimens 3 to 9 were very stable with the ambient side temperature well below the insulation failure temperature of 165^0C (Ambient temperature was 25^0C) throughout the test i.e. no insulation failure. Tests were discontinued after about 3 hours of exposure to the furnace heat. In some of these tests, fire side plasterboards fell-off (Test Specimens 3 and 7 to 9) with thermal bowing deformations towards the furnace while in others the studs suddenly deformed laterally away from the furnace due to the softening and consequent local buckling of hot flanges and associated breaking of plasterboards. Such events can quickly lead to integrity failure or the collapse of the wall with rapid rise in steel stud temperatures. Therefore in these tests, the wall can be considered as failed when the studs reverse their lateral deformation or when the external plasterboards collapse, whichever occurs first. Based on this assumption, Table 2 shows the failure times of test specimens. It indicates that the failure time of Test Specimen 3 (non-insulated LSF wall) is 180 minutes while those of Test Specimens 4 to 6 (Cavity insulted LSF wall) are 125, 145 and 145 minutes, respectively. Hence the use of cavity insulation can be considered detrimental to the fire rating of walls. Table 2 also shows that the failure times of Test Specimens 7 to 9 (External insulted LSF wall) are 198, 200 and 163 minutes, respectively. This shows the superior thermal protection to studs through the use of external insulation than in the case of cavity insulated and non-insulted LSF walls (125 and 180 versus 200 mins).

4. Thermal Behaviour of Non-Load Bearing LSF Walls Using Numerical Studies

This section presents the numerical studies into the thermal behaviour of the tested non-load bearing LSF wall panels and their results. Recently many numerical heat transfer models have been developed [1,22]. There are also many general finite element packages that can be used for thermal analyses. The finite element model employed in this study to predict the thermal behaviour of non-load bearing LSF wall panels was based on SAFIR [7].

4.1. SAFIR

SAFIR is a special purpose finite element program for the analysis of structures under ambient and elevated temperature conditions. It can be used to study the behaviour of one, two and three-dimensional structures. It includes various elements for different idealization and calculation procedures and material models for incorporating stress-strain behaviour. Two standard time-temperature distributions based on ISO834 and ASTM E119 are incorporated into the program. User-defined time-temperature distributions can also be specified. Enthalpy based equation was introduced in SAFIR Version 2002 after using the specific heat equation in the older version of SAFIR (Version 1998). Using specific heat for a material like gypsum that has sudden and short peaks in the temperature-specific heat curve can lead to the solution at a time increment 'stepping over' a peak and thus the solution ignores the energy contained within that peak. If an enthalpy based equation is used then these peaks are always included in the analyses as the enthalpy is calculated by the area under the specific heat versus temperature curve.

4.2. Limitations of SAFIR

Although SAFIR is a very powerful finite element program, the program deficiencies and limitations exist in its ability to model gypsum plasterboard assemblies, and are given in this section. Shrinkage and cracking of the lining are typically taken into account by increasing its thermal conductivity once dehydration has occurred. Ablation is the process when consecutive thin layers of gypsum shed from the plasterboard lining. This has the effect of reducing the cross-sectional thickness of gypsum plasterboard and hence increasing the heat flux across the plasterboard. SAFIR does not allow the user to eliminate the elements from the section to simulate ablation, and therefore, ablation process must be taken into account

through the use of suitable apparent thermal properties of plasterboard. Mass transfer of moisture occurs in plasterboard while heat transfer within plasterboard is highly dependent on its moisture content. The user has the capability to account for moisture content within the material by modifying the respective specific heat curve in the model. However, modelling the moisture movement across the cavity and plasterboards is not incorporated in SAFIR. This phenomenon is generally neglected due to its complexity, and because it only influences the heat transfer across the cavity at temperatures below 120ºC [15].

4.3. GiD Pre- and Post-Processor

GiD is a general purpose pre- and post processor which may be used for a variety of finite element analysis programs. The GiD software package is capable of handling data input, geometry and mesh generation for both thermal and structural SAFIR analyses and can also be used to visualise result files. In this research the GID software was used to create the input file for finite element modelling as well as analysing the model output results.

The geometrical model may be input into GID manually or using Computer Aided Drawing (CAD) software via direct import of DXF drawing file. Figure 9(a) shows GID geometries that were used in this research. All materials embedded in SAFIR may be applied to surface within GID. Properties of user defined materials may also be input and applied to surfaces in a similar manner. SAFIR provided some predefined time-temperature curves such as FISO, F20, F1000, F0, etc. These entire predefined time-temperature curves can be applied directly to a point or a line in the model geometry. FISO was used on the line where the model was exposed to the standard fire curve produced by the furnace while F20 was used on the ambient side (Figure 9(b)). User defined time-temperature curves can also be used in a similar manner. This was adopted to simulate the actual time-temperature curves produced by the furnace in each test.

GID can create either triangular or quadrilateral meshes for 2D calculations. Three-dimensional structures are described by solid elements with 6 or 8 nodes. Figure 9(c) shows the generated mesh of Specimen 8. In order to obtain accurate results, a fine finite element mesh was assigned to the plasterboard (element size is 2mm). Automatic mesh generation was used in developing the finite element models. GID can be used as a post-processor to graphically plot the results contained in the SAFIR analysis output file. In the post-processing

mode GID is capable of displaying thermal contours, plotting the temperature history of identified node/element and for a structural analysis displaying resulting load vectors and structural actions. Figure 9(d) shows the GID with active post-processing interface and temperature contours.

4.4. Thermal Boundary Conditions and Material Properties

The heat flux at the boundary will be calculated from the temperature of the fire curve T_g and the temperature on the surface T_s according to Equation (4).

$$q = h(T_g - T_s) + \sigma\varepsilon(T_g^4 - T_s^4) \quad (4)$$

where q is the total heat flux, ε is the relative emissivity, σ is the Stefan–Boltzmann constant ($5.67E^{-08}W/m^2/K^4$), T_g and T_s are the gas and surface temperatures, respectively.

For fire exposure to the standard cellulosic curve, $T_g = 345\log(8t+1)+20$. Convective heat transfer coefficient (h) is approximately $25 W/m^2K$ on the fire exposed side, and it is 10 W/m^2K on the unexposed side. Emissivity of 0.9 was used for both exposed and unexposed surfaces. Default thermal properties (specific heat and thermal conductivity) for both Type X and Type C gypsum plasterboards within SAFIR are based on Cooper's [12] research, which was based on the work of Sultan [1]. However, the proposed thermal properties in Section 2 were used in this research.

In order to investigate the thermal performance of non-load bearing LSF walls, finite element models of Kolarkar's [5] test wall panels were developed as shown in Figures 10 (a) to (d). Here two voids were created to transfer the heat through radiation and convection. Elements surrounding an internal void were assigned in the counter clockwise direction. The developed finite element models were validated using the results obtained from fire tests of non-load bearing LSF walls in [5].

Heat transfer in the cavities (void) was defined by radiation and convection between the boundaries of the cavity. In the numerical model, radiation and convection coefficients were used to simulate the radiation and convection heat transfer in the cavity. The specific heat of air was assumed to be negligible in the numerical model. The time step used in the analyses was 1s.

4.5. Validation of Finite Element Models Using Fire Test Results

It is necessary to validate the developed finite element models for the thermal analyses of non-load bearing LSF walls. This was achieved by comparing the time-temperature profiles with the corresponding fire test results of non-load bearing LSF walls [5]. Figures 11(a) to (h) show the finite element analysis (FEA) results in the form of temperature versus time for non-load bearing LSF wall specimens and compare them with corresponding test results. The average temperature profiles of the three studs were considered in the comparison of test and FEA results. These figures indicate that the developed finite element models predict the time-temperature profiles of non-load bearing LSF walls with good accuracy.

Finite element analyses clearly show that the temperature gradients across the steel studs and associated thermal bowing effects are larger when cavity insulation is used in comparison to other cases (Figures 11(a) to (e)). Hence it is considered that the use of cavity insulation is detrimental to the fire rating of walls as also shown by fire tests. Figures 11(f) to (h) show that the new composite LSF wall panels using external insulation lead to reduced temperatures in steel studs at any given time and a more uniform temperature distribution across their cross-sections, thus producing minimum early lateral deformation (thermal bowing). For example, the results show that in Specimen 4 with glass fibre cavity insulation the hot (HF) and cold flange (CF) temperatures are 570^{o}C and 290^{o}C after 120 minutes while in Specimen 7 with glass fibre external insulation they are 360^{o}C and 260^{o}C (Figures 11(c) and (f)). Hence it is clear that the use of external insulation is able to provide much greater thermal protection to LSF steel studs than cavity insulation. All of these findings thus confirm the observations made in Kolarkar's fire tests [5].

It should be noted that non-load bearing LSF walls exposed to fires are affected by processes not described by heat transfer such as ablation of plasterboard and insulation, migration of moisture vapours and penetration of cool ambient air or hot furnace gases into the cavity. These processes were taken into account through the use of suitable apparent thermal properties of plasterboard (Section 2).

In summary, the comparisons between FEA and fire test results reported here have established the validity of the finite element models in simulating the thermal behaviour of

small scale non-load bearing LSF walls and the accuracy of the values used for relative emissivity, convective coefficient and other thermal properties. The results from FEA also produced valuable time-temperature data and an improved understanding of the thermal performance of non-load bearing LSF wall panels using cavity and external insulations. Figure 12 shows the temperature distributions across the cross-section of Specimen 8 (Rockwool external insulation). Test temperature results were higher than FEA results when the plasterboards started to fall off. Hence finite element models developed here are considered to be able to predict the time-temperature profiles of LSF walls with good accuracy until the commencement of plasterboard fall-off. Since the time-temperature profiles from small scale tests are likely to be different to those from full scale tests, further validation of finite element models might be needed using full scale test data.

5. Effects of Various Parameters on the Thermal Behaviour of Non-Load Bearing LSF Wall Panels

5.1. Geometry of Cold-formed Steel Stud Section

In order to investigate the effect of the geometry of cold-formed steel stud section on the thermal behaviour of non-load bearing LSF walls, further finite element analyses were conducted. LSF wall panels made of 90x40x15x1.15 LSB and 90x40x15x1.15 LCB (Test Specimen 1) with single plasterboard on both sides of steel studs were considered. Here a lipped channel (LCB) section and a LiteSteel beam (LSB) section were considered. The LiteSteel beam (LSB) is a new cold-formed steel hollow flange channel beam produced using a patented manufacturing process involving simultaneous cold-forming and dual electric resistance welding. Figure 13 shows the time-temperature profiles of LSB and LCB wall panels. It indicates that the geometry of the cold-formed steel stud section does not have a significant effect on the temperature distributions in LSF wall panels.

5.2. Steel Stud Depth

In order to investigate the depth of cold-formed steel studs on the thermal behaviour of non-load bearing LSF walls, further finite element analyses were conducted. LSF wall panels made of 150x40x15x1.15 LCB and 90x40x15x1.15 LCB (Test Specimen 1) with single plasterboard on both sides of steel studs were investigated. Figure 14 shows the time-temperature profiles of 150x40x15x1.15 LCB and 90x40x15x1.15 LCB wall panels. It

indicates that the depth of the cold-formed steel member does not have a significant effect on the temperature distributions in LSF wall panel systems.

5.3. Real Design Fire Curves

The standard fire curve was originally developed based on wood fuel burning furnaces and was then slightly modified to represent the gas fired furnace temperatures. However, this approach was not based on fire severities in real buildings. No significant change has been made to the standard time-temperature curve, which is still being used to calculate the Fire Resistance Ratings (FRR) of assemblies. Standard time-temperature curve does not represent the modern accessories in typical residential and commercial buildings, where they incorporate both traditional wooden furniture and modern items such as cushion furniture, mattresses, fabric coated partitions and many other items that make use of thermoplastic materials. These modern synthetic materials increase both the speed of fire growth and peak heat release rate, thus increasing the fire severity beyond the standard curve used to obtain the FRR times. Hence construction elements may not ensure safe evacuation or offer the required life safety for occupants. Therefore there is a need to obtain the true fire resistance rating times under real fire conditions. The standard fire curve in ISO834 does not represent the true fire conditions. Therefore finite element analyses were performed using the recently developed realistic design fire curves in [23]. They were conducted using the finite element model described in Section 4 and the proposed thermal properties in Section 2.

Two Eurocode parametric curves (EU1 and EU2) were considered in the numerical studies reported in this section. EU1 and EU2 curves represent the opening factors of 0.02 (EU1) and 0.12 (EU2) as they cover the entire range, and are conservative. Also EU1 (0.02) and EU2 (0.12) would be the ideal time-temperature curves for the investigation of non-load bearing LSF wall panels for real building fires as they include a rapid development (EU2) and a prolonged development (EU1) fire falling between the two extremes. Figure 15 shows these two Eurocode parametric curves developed for dwellings based on a fuel load density of 1138.00 MJ/m^2 [23,24]. Figures 16(a) and (b) show the finite element analysis results in the form of temperature versus time for a non-load bearing LSF wall panel (Test Specimen 8 with external rockwool insulation) under real design fire conditions [24] and compare them with those under standard fire conditions. Figure 16(a) shows that the time-temperature profiles of non-load bearing LSF wall panels under real design fire (EU1) are much higher

than those under standard fire while Figure 16(b) shows that the time-temperature profiles of non-load bearing LSF wall panels under real design fire EU2 are lower than those under standard fire. It is clear from Figure 16(a) that real design fires such as EU1 can cause severe damage to LSF wall panels than standard fires. However, real design fire such as EU2 will not cause severe damage to LSF wall panels than standard fires (Figure 16(b)). Since EU2 real design fire has rapid development fire for a short period of time (25 min), temperatures of steel used in Test Specimen 8 under this fire are lower than those under standard fires. Finite element analyses gave the same findings for cavity insulated LSF panels under real design fires considered here.

6. Conclusions

This paper has presented the details of a numerical study on the thermal performance of non-load bearing LSF wall panels that included both the conventional cavity insulated wall systems and the new composite panel systems. It included the details of the developed finite element models of non-load bearing LSF wall panels, the thermal analysis results from SAFIR under standard fire conditions and their comparisons with fire test results obtained by Kolarkar [5]. A good comparison with fire test results showed that accurate finite element models can be developed and used to simulate the thermal behaviour of small scale non-load bearing LSF wall panels with varying configurations of cavity and external insulations and plasterboards. A good agreement was obtained until the commencement of plasterboard fall-off. For this purpose the proposed apparent thermal properties of plasterboard, insulation materials and steel given in this paper should be used.

Experimental and numerical studies showed that the use of cavity insulation was detrimental to the fire rating of walls. It not only led to higher temperatures in the steel studs, but also to larger temperature gradients across their depth and increased thermal bowing effects. In contrast, the use of external insulation led to lower temperatures and a more uniform temperature distribution in the steel stud cross-sections at any given time, thus providing greater thermal protection to the walls. Finite element analysis results showed that the shape and depth of the cold-formed steel stud cross-sections did not have a significant effect on the temperature distributions in LSF wall panels. The use of real design fire conditions based on Eurocode parametric curves in the numerical studies showed that some real building fires can

cause severe damage to LSF wall panels than the standard fire specified in various fire codes while other real building fires are not as severe as the standard fire.

Acknowledgements

The authors would like to thank Australian Research Council for their financial support and the Queensland University of Technology for providing the necessary facilities and support to conduct this research project.

References

1. Sultan, M. A. (1995), Effect of Insulation in the Wall Cavity on the Fire Resistance Rating of Full-Scale Asymmetrical (1 x 2) Gypsum Board Protected Wall Assemblies, Proceedings of the International Conference on Fire Research and Engineering, Orlando, FL, Lund D. P. (Ed.), Society of Fire Protection Engineers, Boston, MA, pp. 545-550.
2. Kodur, V.R. and Sultan, M.A. (2001), Factors Governing Fire Resistance of Load Bearing Steel Stud Walls, Proc. of the 5th AOSFST International Conference, Newcastle, Australia, pp.1-2.
3. Feng, M., Wang, Y.C. and Davies, J.M. (2003), Thermal Performance of Cold-formed Thin-walled Steel Panel Systems in Fire, Fire Safety Journal, Vol.38, pp.365–394.
4. Kolarkar, P. and Mahendran, M. (2008), Thermal Performance of Plasterboard Lined Steel Stud Walls, Proc. of the 19th International Specialty Conference on Cold-Formed Steel Structures, St. Louis, Missouri, USA, pp.517-530.
5. Kolarkar, P. (2010), Structural and Thermal Performance of Cold-formed Steel Stud Wall Systems under Fire Conditions, PhD Thesis, Queensland University of Technology, Brisbane, Australia.
6. Keerthan, P. and Mahendran, M. (2010), Numerical Studies of Gypsum Plasterboards under Fire Conditions, Research Report, Queensland University of Technology, Brisbane, Australia.
7. Franssen, J.M., Kodur, V.K.R. and Masson, J. (2004), User's Manual for SAFIR 2004: A Computer Program for Analysis of Structures Submitted to the Fire, University of De Leige, Institute Du Genie Civil, Liege, Belgium.

8. Thomas, G.C. (2002), Thermal Properties of Gypsum Plasterboard at High Temperatures, Fire and Materials, Vol.26, pp.37–45.
9. Thomas, G.C. (2010), Modelling Thermal Performance of Gypsum Plasterboard-lined Light Timber Frame Walls using SAFIR and TASEF, Fire and Materials, Accepted, DOI: 10.1002/fam.1026.
10. Wakili, K.G., Hugi, E., Wullschleger, L. and Frank, T.H. (2007), Gypsum Board in Fire—Modelling and Experimental Validation, Journal of Fire Sciences, Vol.25, pp.267–282.
11. Manzello, S.L., Richard, G.G., Scott, R.K. and David B.L. (2008), Influence of Gypsum Board Type (X or C) on Real Fire Performance of Partition Assemblies, Fire and Materials, Vol.31, pp.425-442.
12. Cooper, L.Y. (1997), The Thermal Response of Gypsum-Panel/Steel Stud Wall Systems Exposed to Fire Environments – A Simulation for the use in Zone-Type Fire Models, NIST Report NISTIR 6027, Building and Fire Research Laboratory, National Institute of Standards and Technology, Gaithersburg, USA.
13. Keerthan, P. and Mahendran, M. (2011), Thermal Performance of an Innovative Composite Panel under Fire Conditions Using Numerical Studies, Research Report, Queensland University of Technology, Brisbane, Australia.
14. Takeda, H. and Mehaffy, J.R. (1998), Wall 2D: A Model for Predicting Heat Transfer Through Wood-Stud Wall Exposed to Fire, Fire and Material, Vol.22, pp.133-140.
15. Thomas, G.C. (1997), Fire Resistance of Light Timber Framed Walls and Floors, Fire Engineering Research Report 97/7, University of Canterbury, Christchurch, New Zealand.
16. Alfawakhiri, F. (2001), Behaviour of Cold-Formed Steel-Frames Walls and Floors in Standard Fire Resistance Tests, PhD Thesis, Department of Civil and Environmental Engineering, Carleton University, Canada.
17. EN 1993-1-2 (1995) Eurocode 3: Design of steel structures - Part 1-2: General Rules - Structural Fire Design, European Committee for Standardization, Brussels.
18. Buchanan, A.H. (2001), Fire Engineering Design Guide. Centre for Advanced Engineering, University of Canterbury, Christchurch, New Zealand.
19. Standards Australia (SA) (2005), AS 1530.4 Methods for fire tests on building materials, components and structures, Part 4: Fire-resistance tests of elements of building construction, 2005, Sydney, Australia.

20. ISO 834 (1999), Fire Resistance Tests – Elements of Building Construction, International Organisation for Standardisation, Switzerland.
21. ASTM El 19 (2000), Standard Methods of Fire Tests of Building Construction and Materials, American Society for Testing and Materials, Philadelphia, USA.
22. Franssen, J.M. (2005), SAFIR - A Thermal/Structural Program Modelling Structures under Fire, Engineering Journal, Vol.42, pp.143–158.
23. Ariyanayagm, A. (2010), Structural and Thermal Behaviour of Light Gauge Steel Frame Wall Panels Exposed to Real Fires, PhD Report, Queensland University of Technology, Brisbane, Australia.
24. ENV 1991-1-2 (2002) Eurocode 1: Actions on Structures, Part 1-2: Actions on Structures Exposed to Fire, European Committee for Standardization, Brussels.

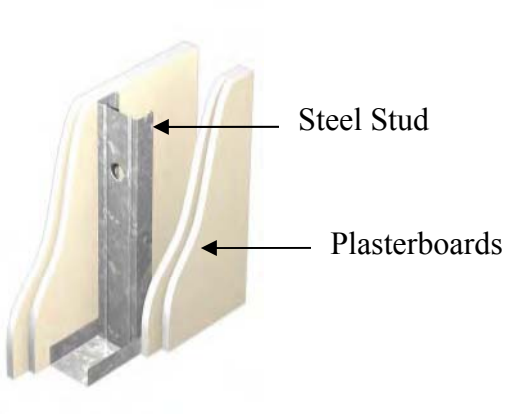

Figure 1: LSF Wall with Gypsum Plasterboard Lining

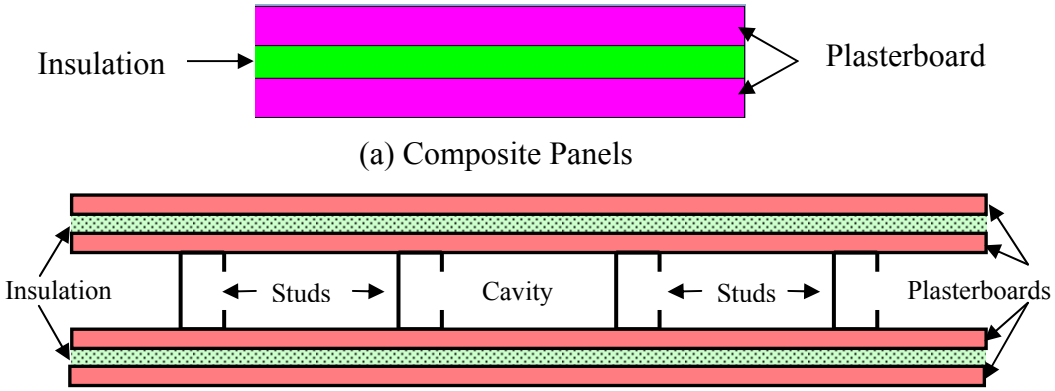

Figure 2: Composite Panels and LSF Wall Panels [4]

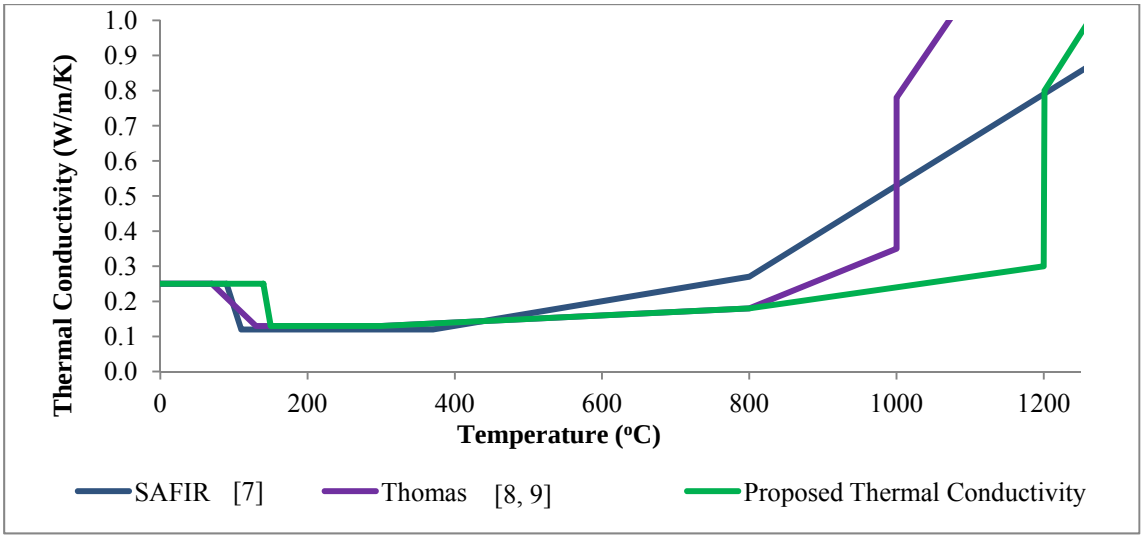

(a) Thermal Conductivity

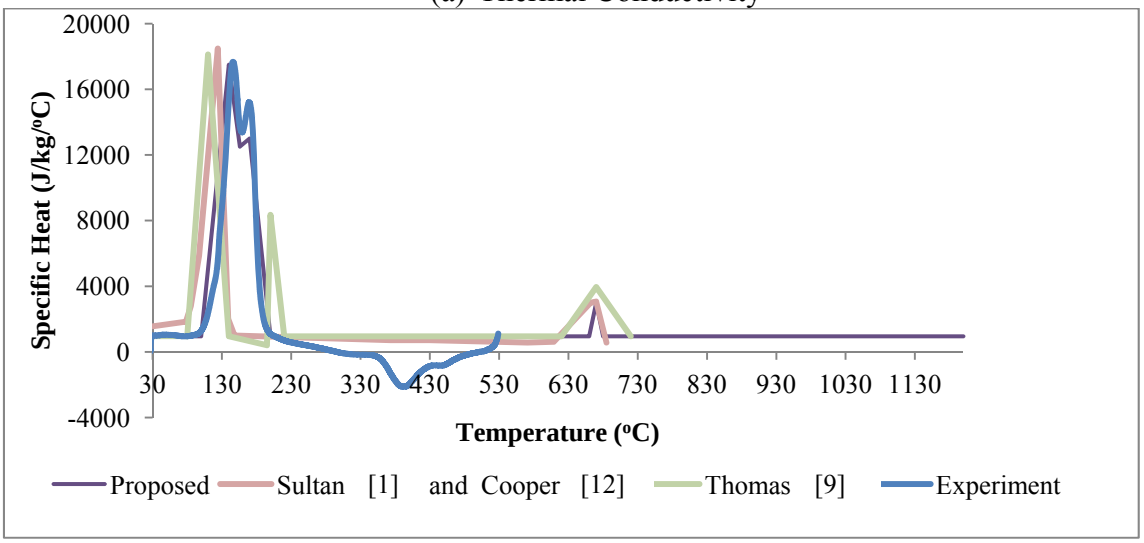

(b) Specific Heat Incorporating the Third Peak Based on Test Results

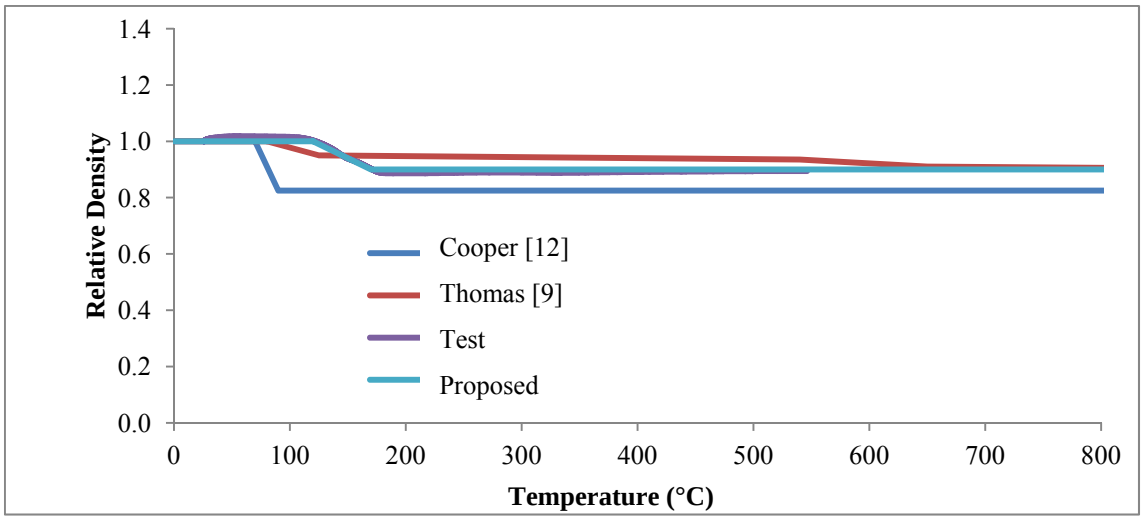

(c) Relative Density of Plasterboard

Figure 3: Proposed Thermal Properties of Plasterboard

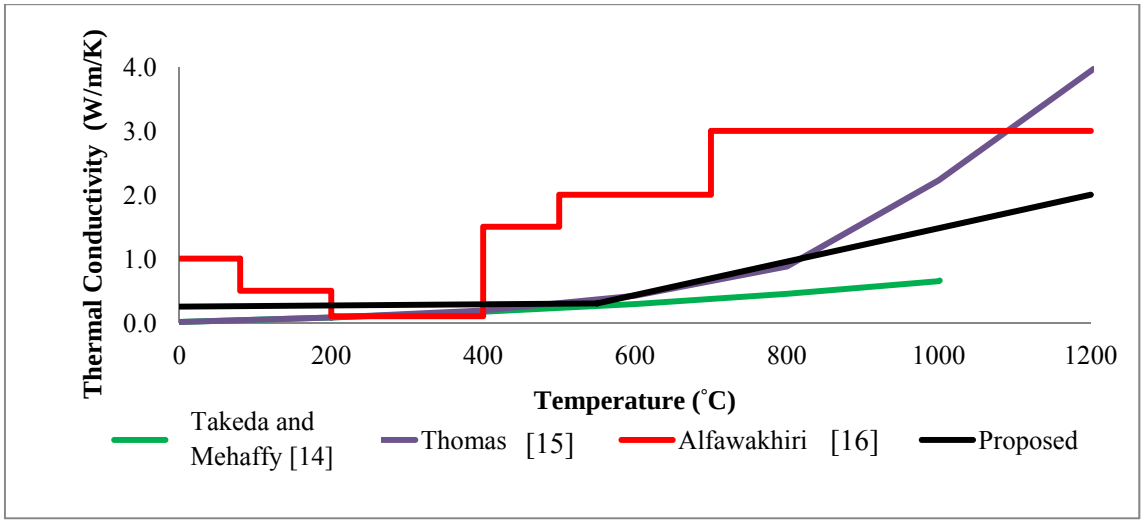

(a) Rockwool

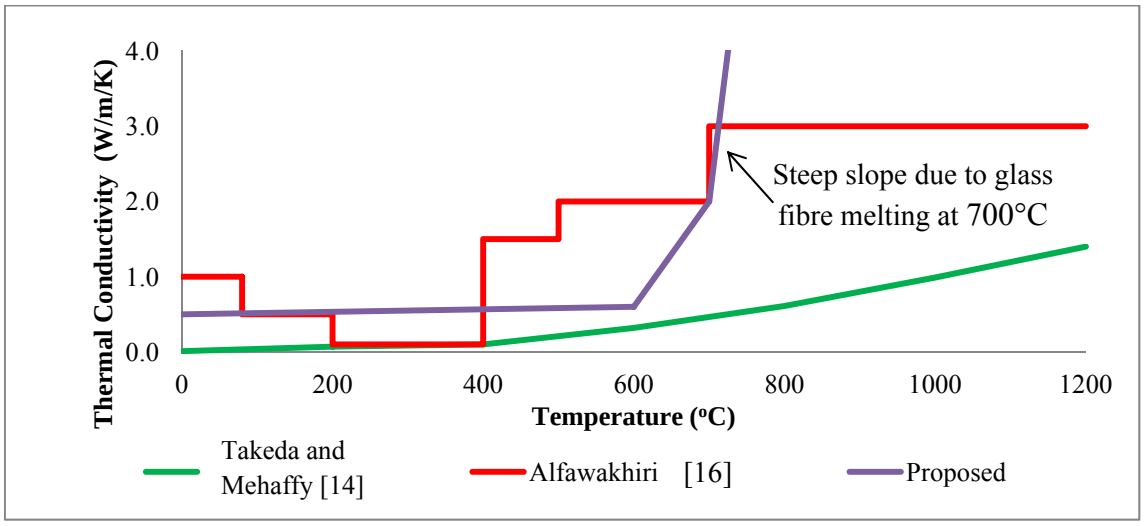

(b) Glass Fibre

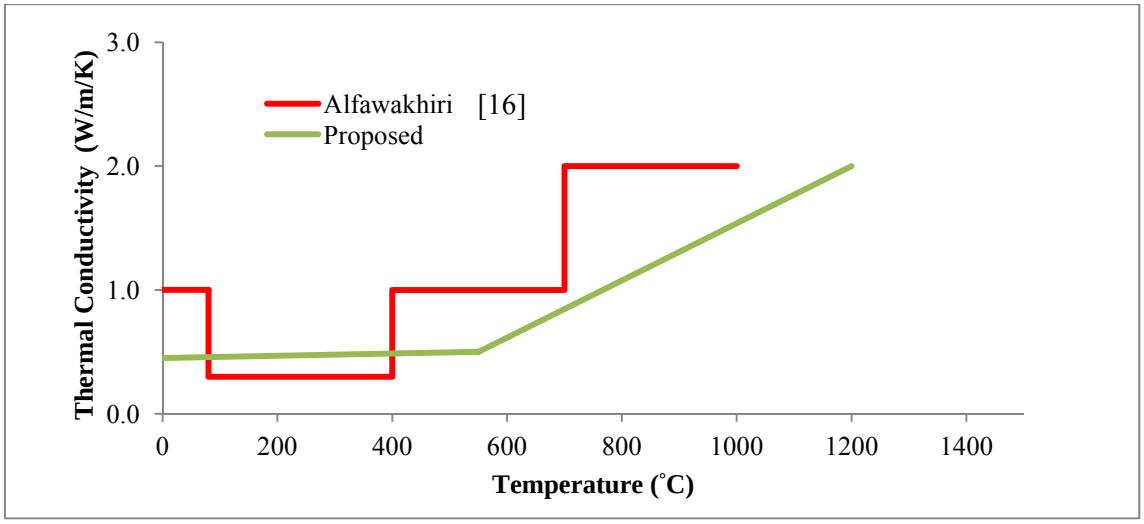

(c) Cellulose Fibre

Figure 4: Proposed Thermal Conductivity of Insulations

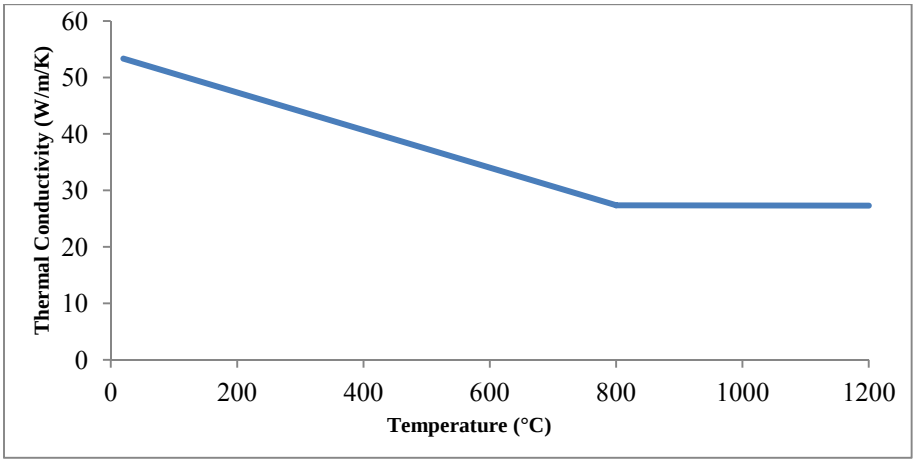

(a) Thermal Conductivity

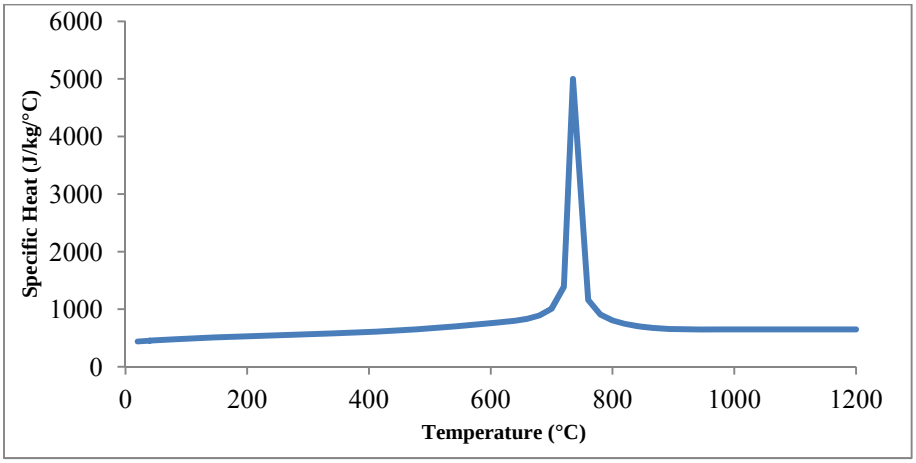

(b) Specific Heat

Figure 5: Plot of Thermal Properties of Steel versus Temperature [17]

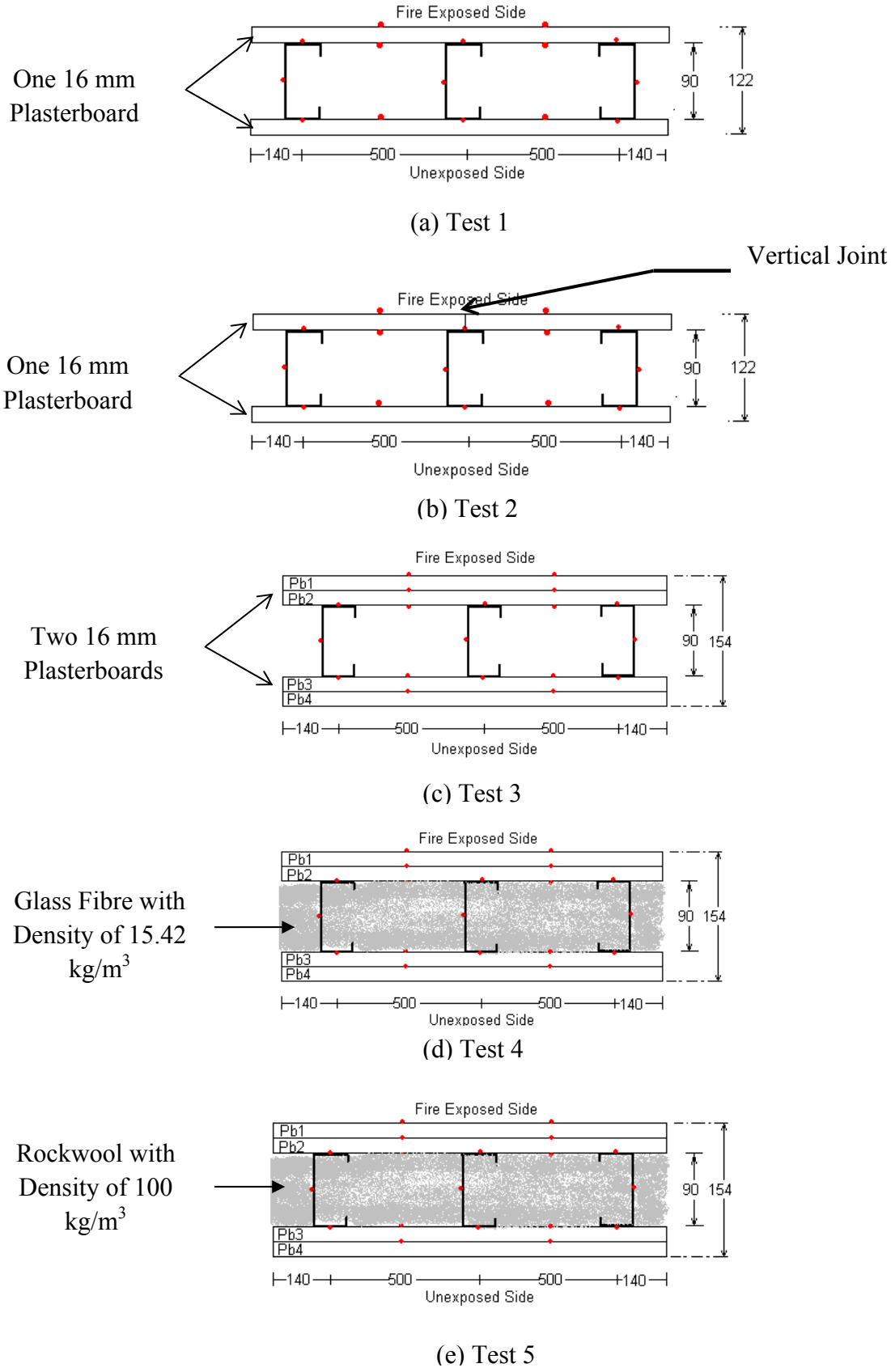

Figure 6: Schematic Diagrams of LSF Wall Test Specimens [5]

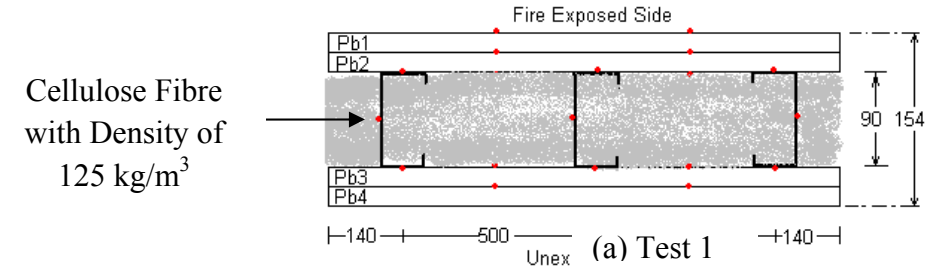

(a) Test 1

(f) Test 6

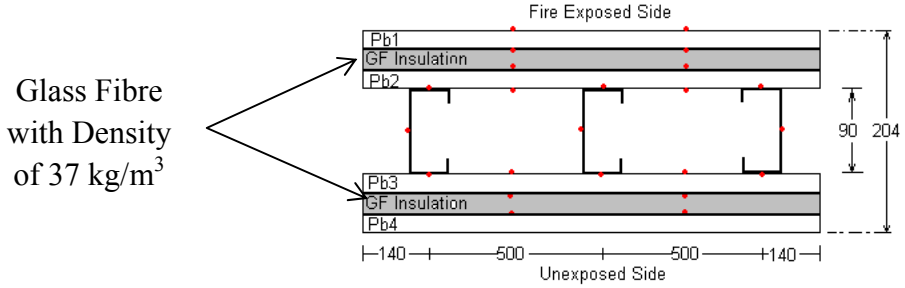

(g) Test 7

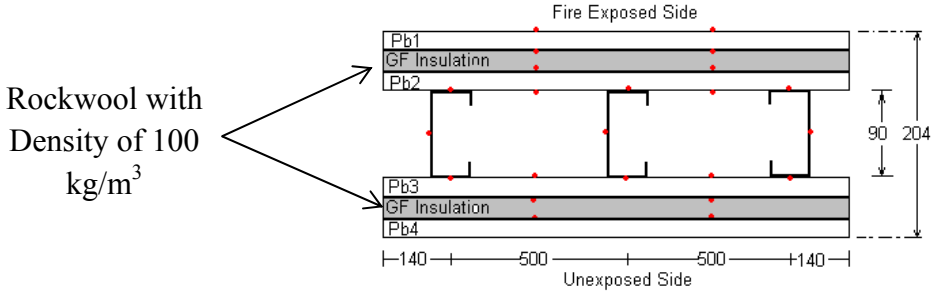

(h) Test 8

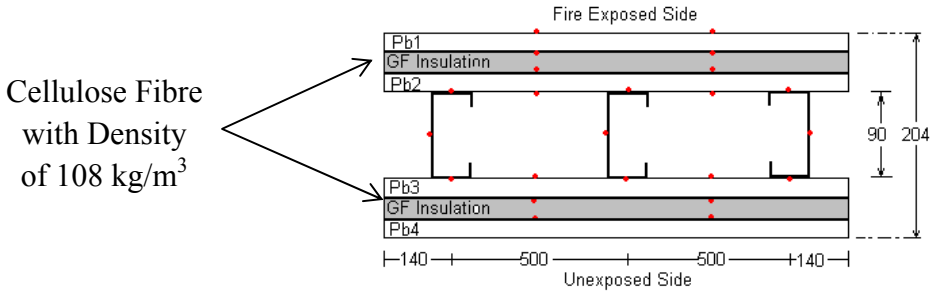

(i) Test 9

Figure 6: Schematic Diagram of LSF Wall Test Specimens [5]

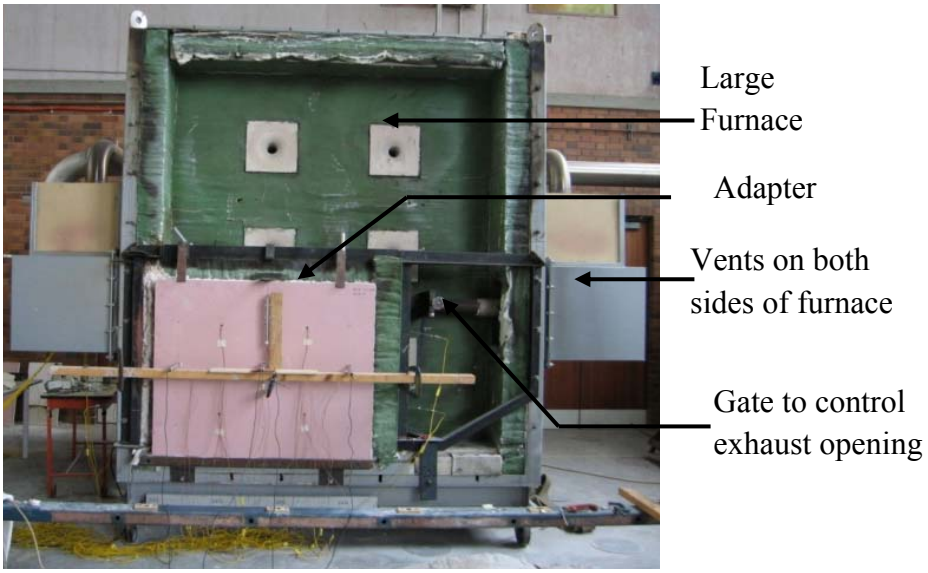

Figure 7: Test Set-up for Non-load Bearing LSF Wall Panels [5]

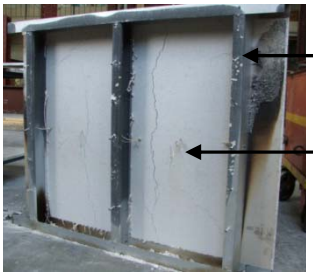

(a) Specimen 3 (No Cavity Insulation)

(b) Specimen 4
(Glass Fibre Cavity Insulation)

(c) Specimen 5
(Rockwool Cavity Insulation)

(d) Specimen 6
(Cellulose Cavity Insulation)

(e) Specimen 7
(Glass Fibre External Insulation)

(f) Specimen 8
(Rockwool External Insulation)

(g) Specimen 9
(Cellulose Fibre External Insulation)

Figure 8: Test Specimens 3 to 9 after the Fire Test [5]

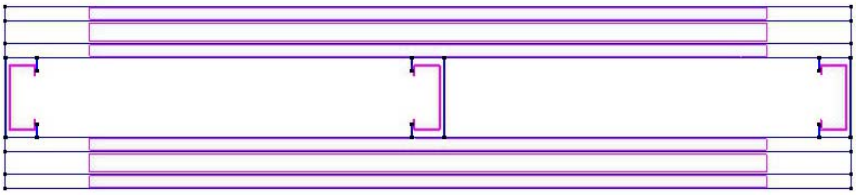

(a) Typical GID Geometry (Specimen 8)

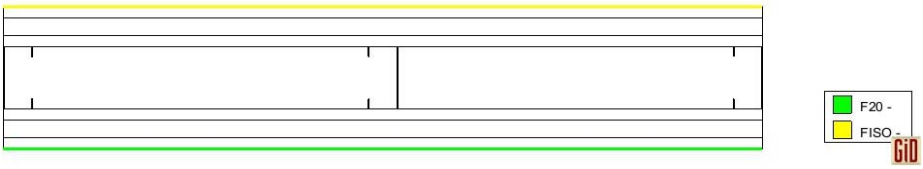

(b) Test Specimen 8 with Thermal Boundary Conditions

F20 = Temperature at 20^{o}C

FISO = Standard Time-Temperature curve according to AS 1530.4

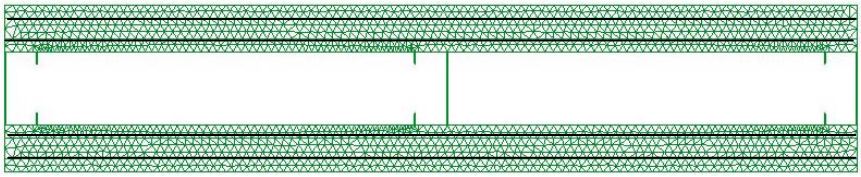

(c) Generated Finite Element Mesh of Test Specimens (Specimen 8)

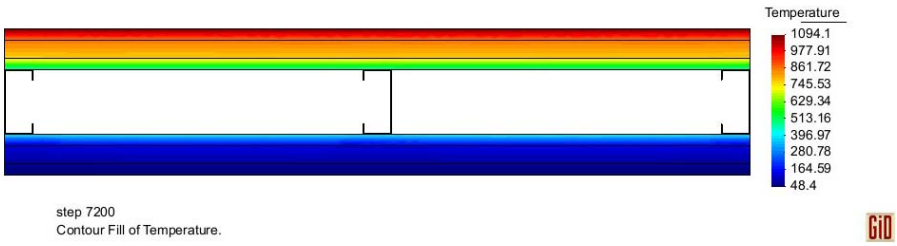

(d) GID Post-Processing Interface with Temperature Contours Active

Figure 9: Finite Element Modelling of LSF Wall Panels

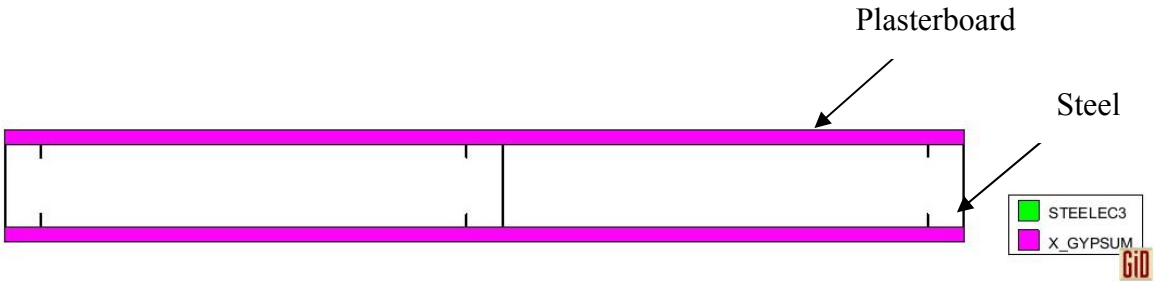

(a) Test Specimen 1

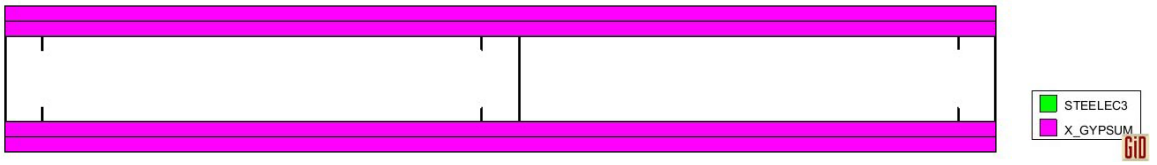

(b)Test Specimen 3

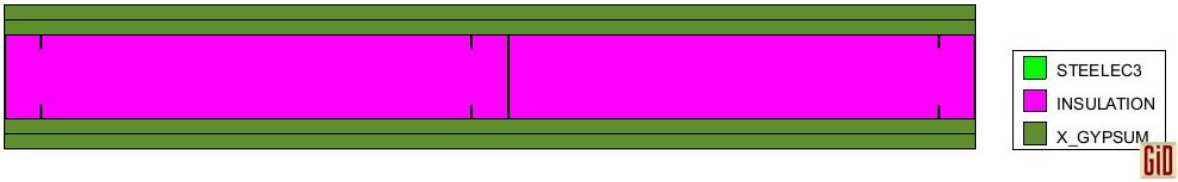

(c) Test Specimens 4 to 6

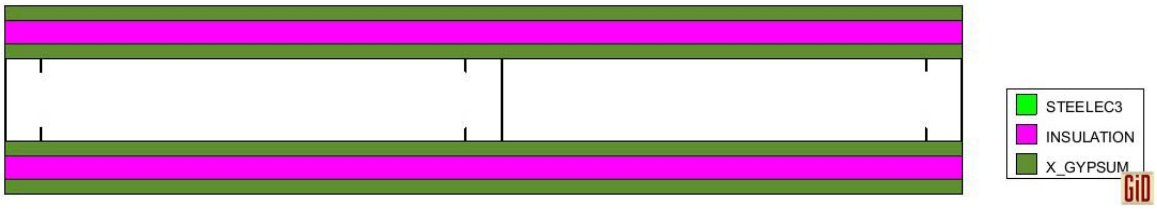

(d) Test Specimens 7 to 9

Figure 10: Finite Element Models of LSF Wall Test Specimens

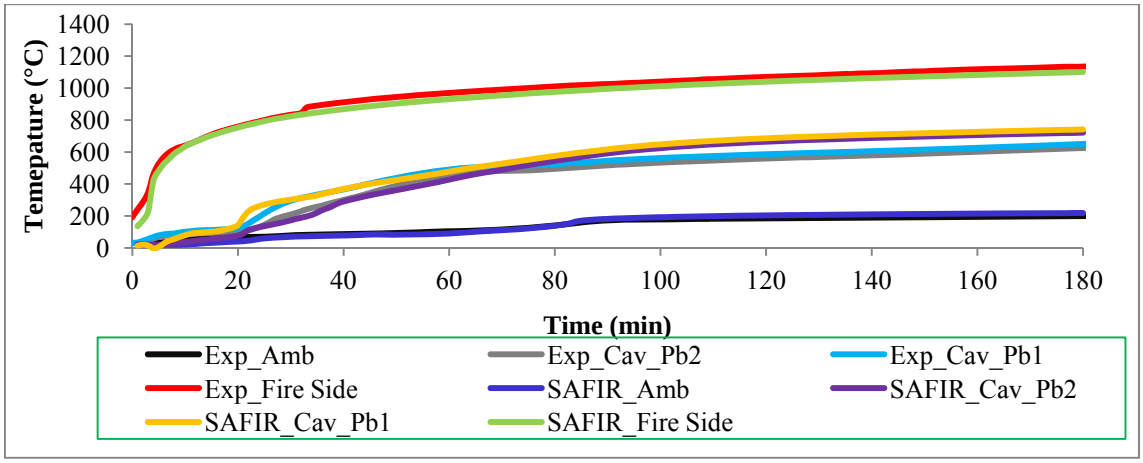

(1) Plasterboard

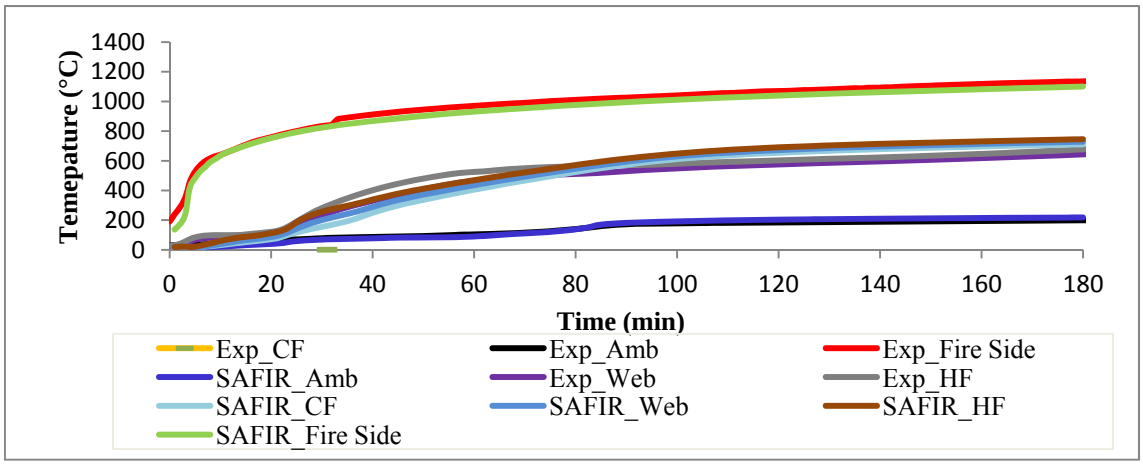

(2) Steel

(a) Test Specimen 1 (single plasterboard with no cavity insulation)

Figure 11: Time-Temperature Profiles of Test Specimens

Note:

HF, Web, CF: Hot Flange, Web and Cold Flange of Steel Stud

Cav-Pb1: Cavity facing surface of Plasterboard 1

Cav-Pb2: Cavity facing surface of Plasterboard 2

Other symbols are similarly defined when there were four plasterboards (Pb3 & Pb4) – Fig.6

Amb: Unexposed surface

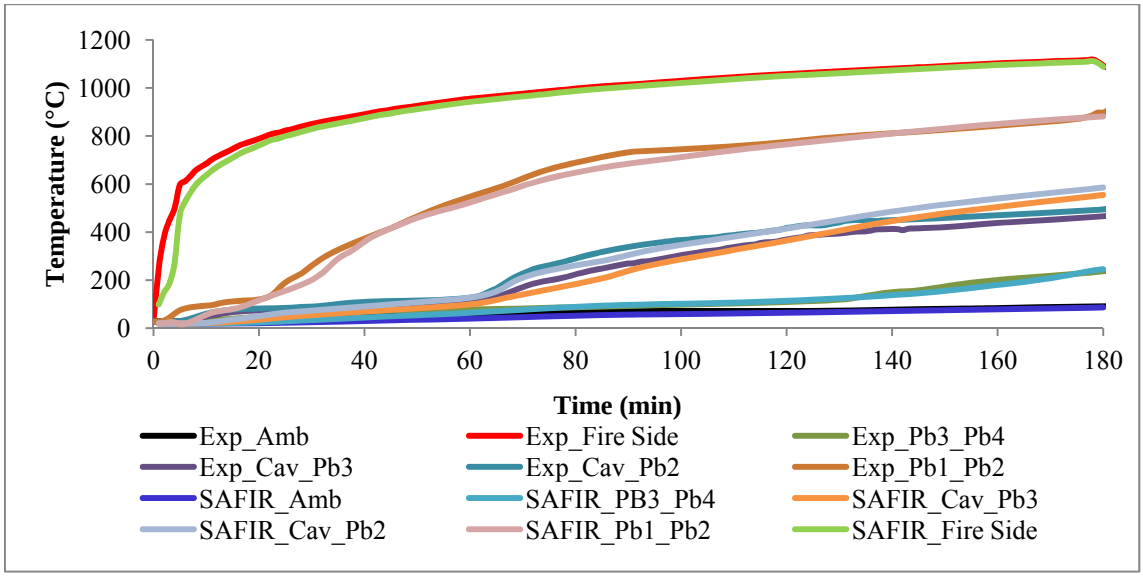

(1) Plasterboard

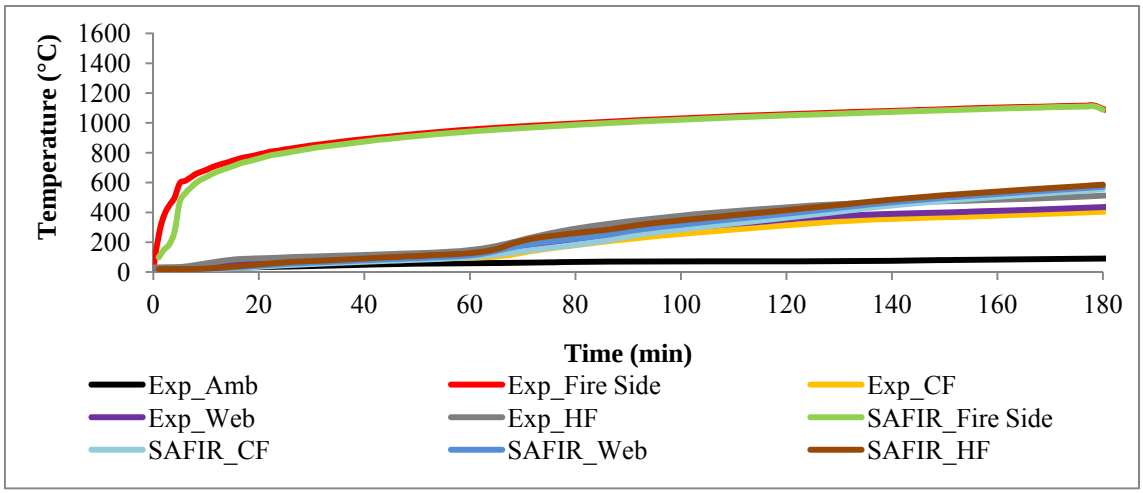

(2) Steel

(b) Test Specimen 3 (double plasterboards with no cavity insulation)

Figure 11: Time-Temperature Profiles of Test Specimens

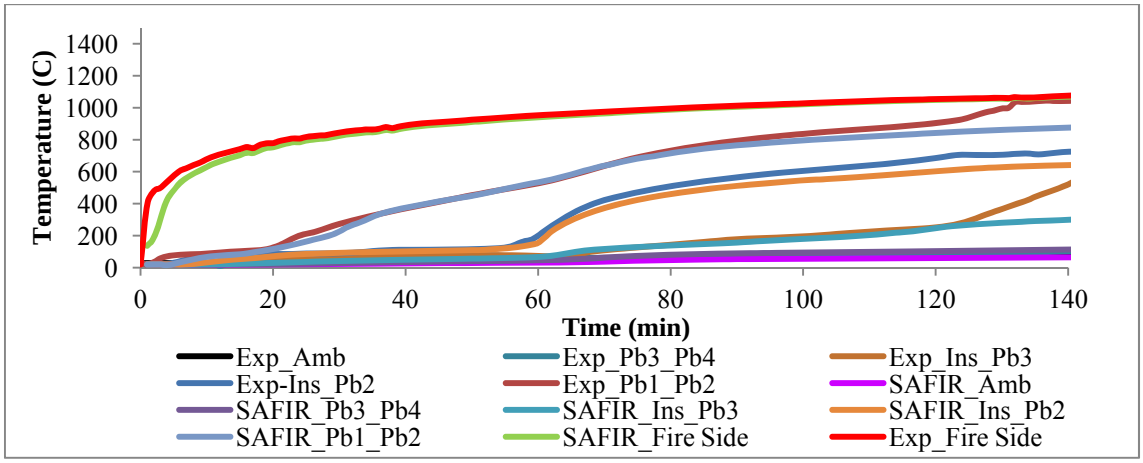

(1) Plasterboard and Insulation

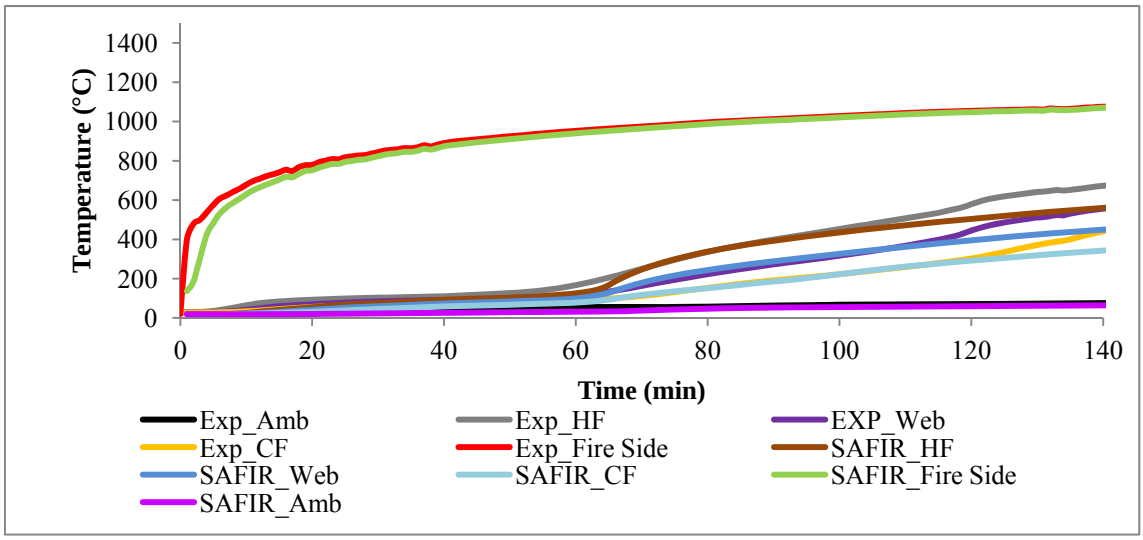

(2) Steel

(c) Test Specimen 4 (glass fibre cavity insulation)

Figure 11: Time-Temperature Profiles of Test Specimens

Note:

Pb1-Pb2: Interface between Plasterboards 1 and 2

Pb3-Pb4: Interface between Plasterboards 3 and 4

Ins-Pb2: Interface between Plasterboard 2 and Insulation

Ins-Pb3: Interface between Insulation and Plasterboard 3

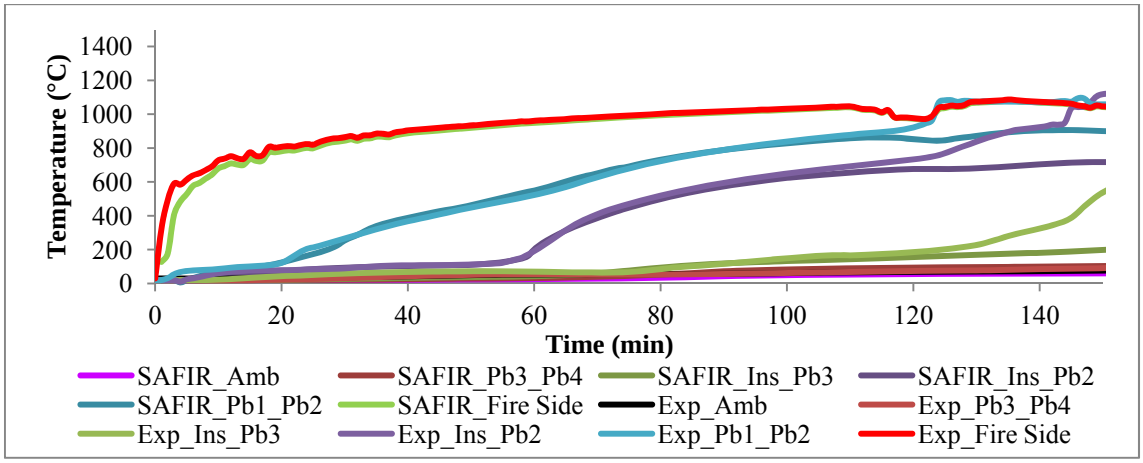

(1) Plasterboard and Insulation

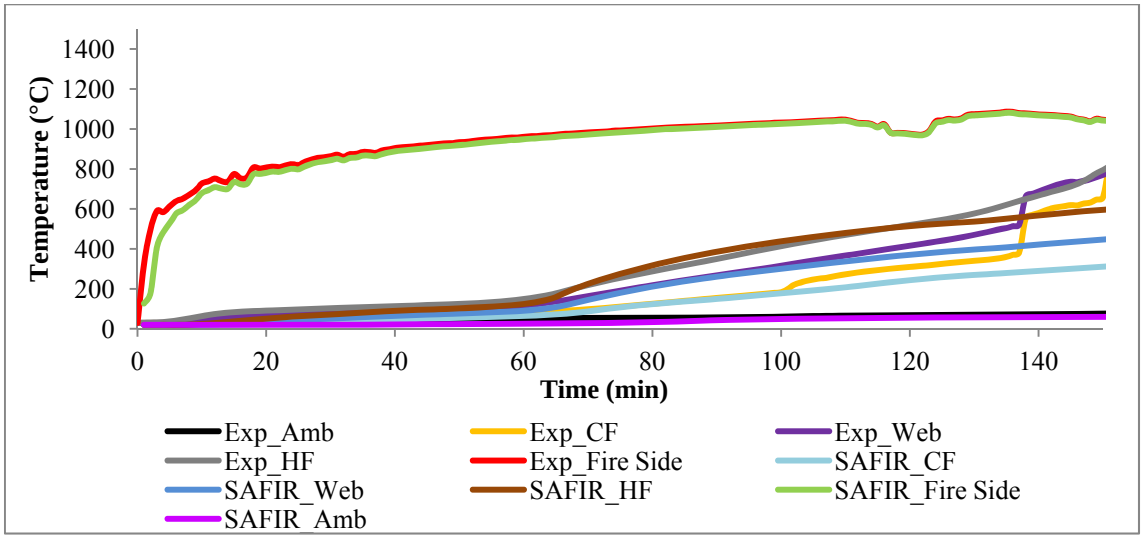

(2) Steel

(d) Test Specimen 5 (rockwool cavity insulation)

Figure 11: Time-Temperature Profiles of Test Specimens

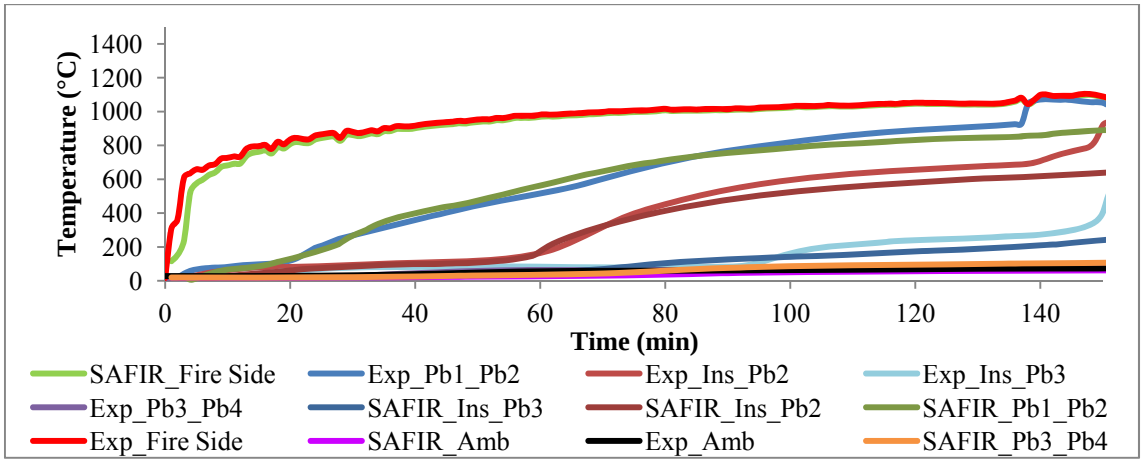

(1) Plasterboard and Insulation

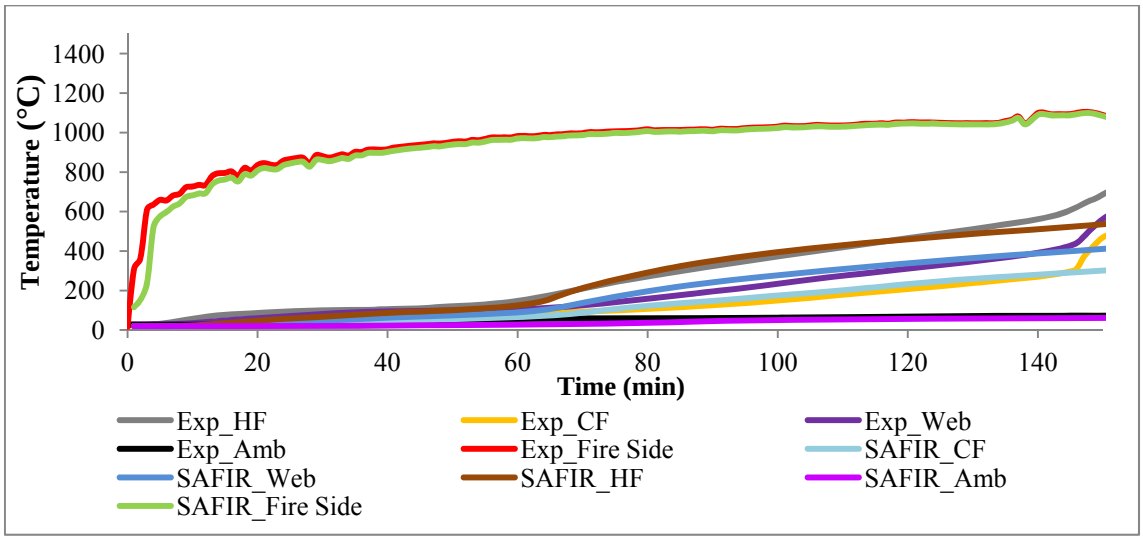

(2) Steel

(e) Test Specimen 6 (cellulose fibre cavity insulation)

Figure 11: Time-Temperature Profiles of Test Specimens

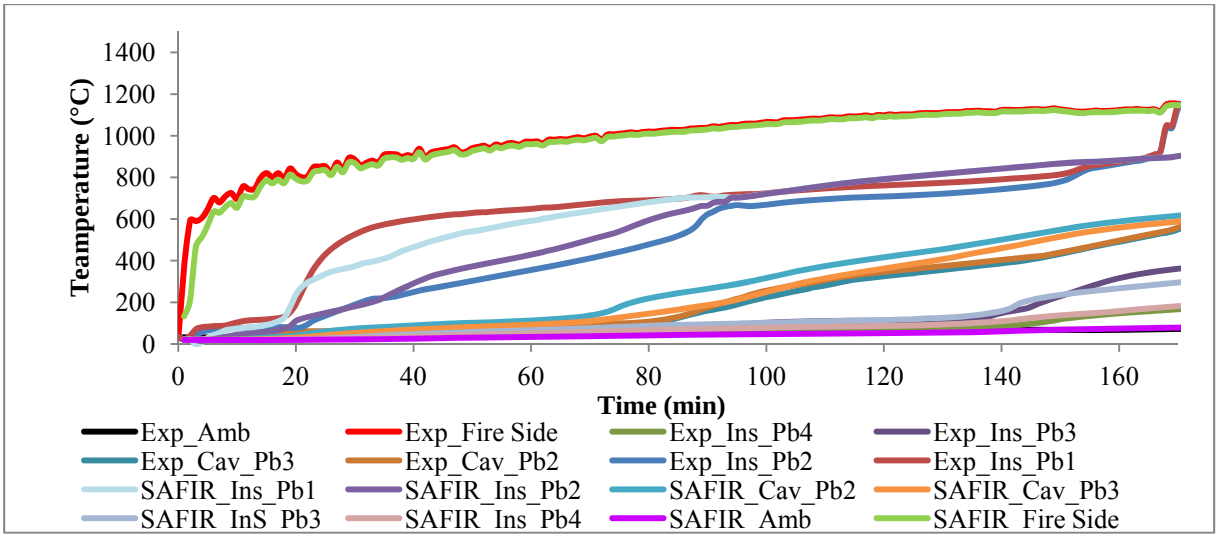

(1) Plasterboard and Insulation

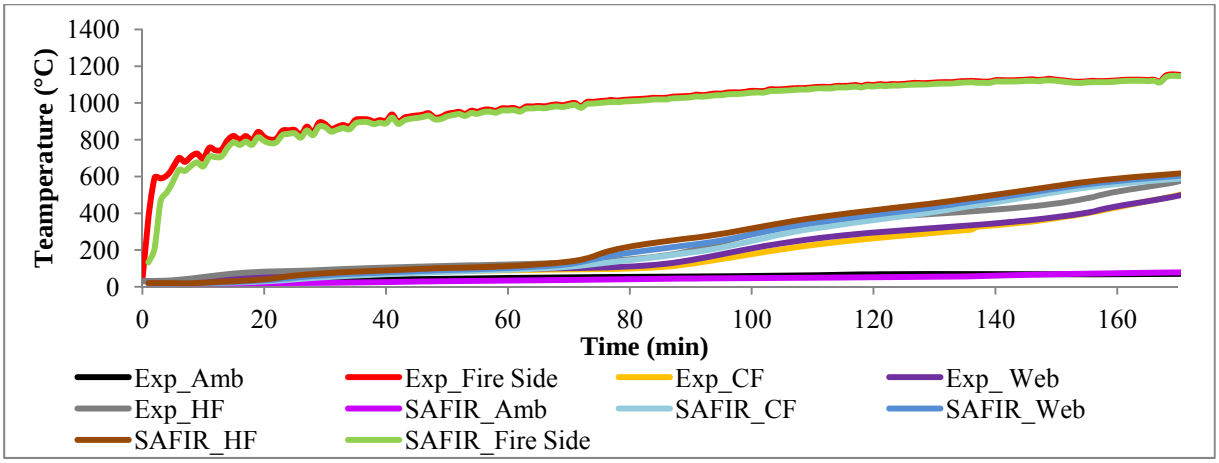

(2) Steel

(f) Test Specimen 7 (glass fibre external insulation)

Figure 11: Time-Temperature Profiles of Test Specimens

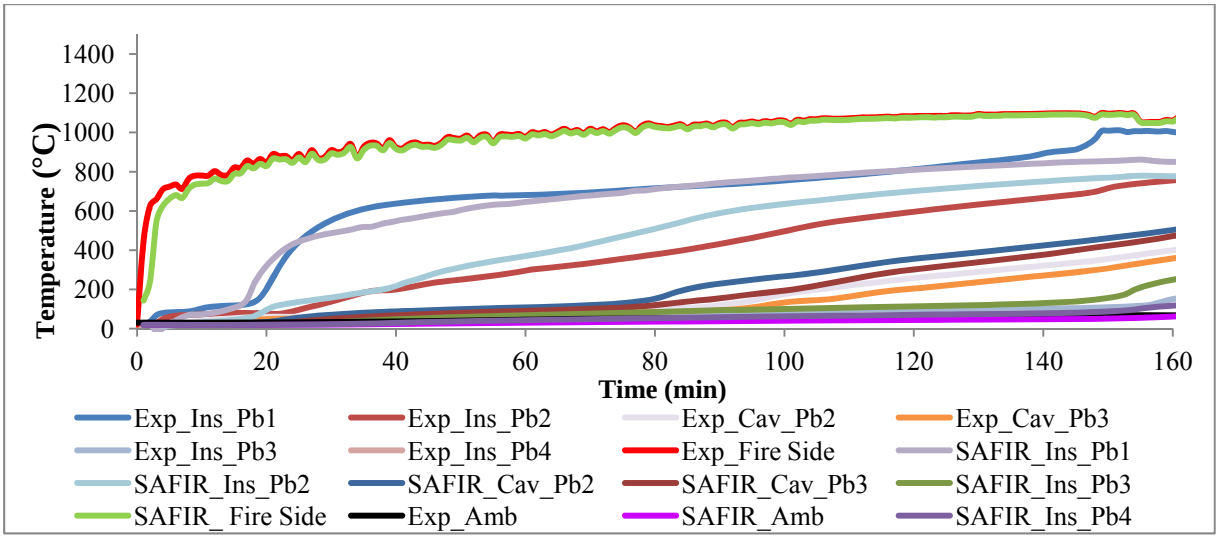

(1) Plasterboard and Insulation

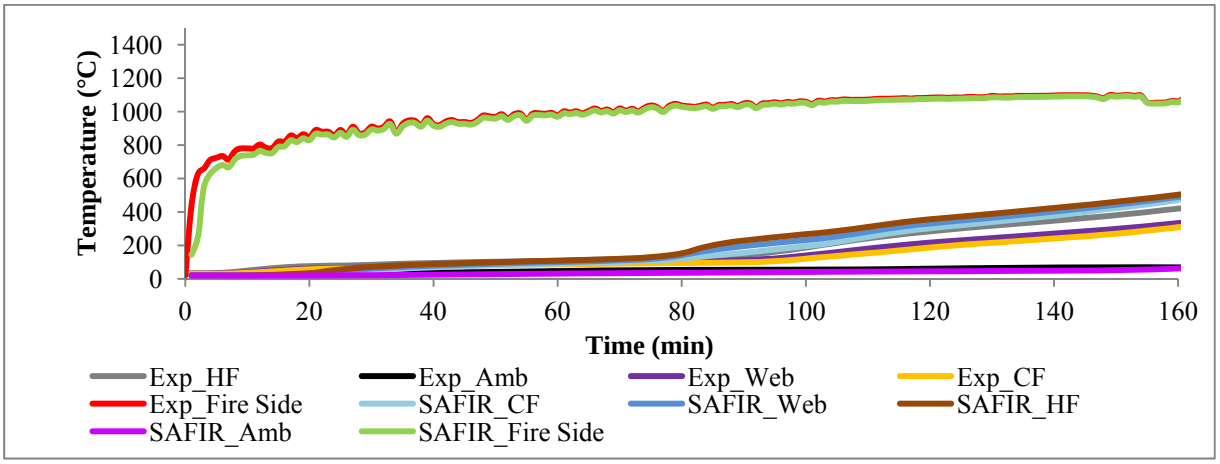

(2) Steel

(g) Test Specimen 8 (rockwool external insulation)

Figure 11: Time-Temperature Profiles of Test Specimens

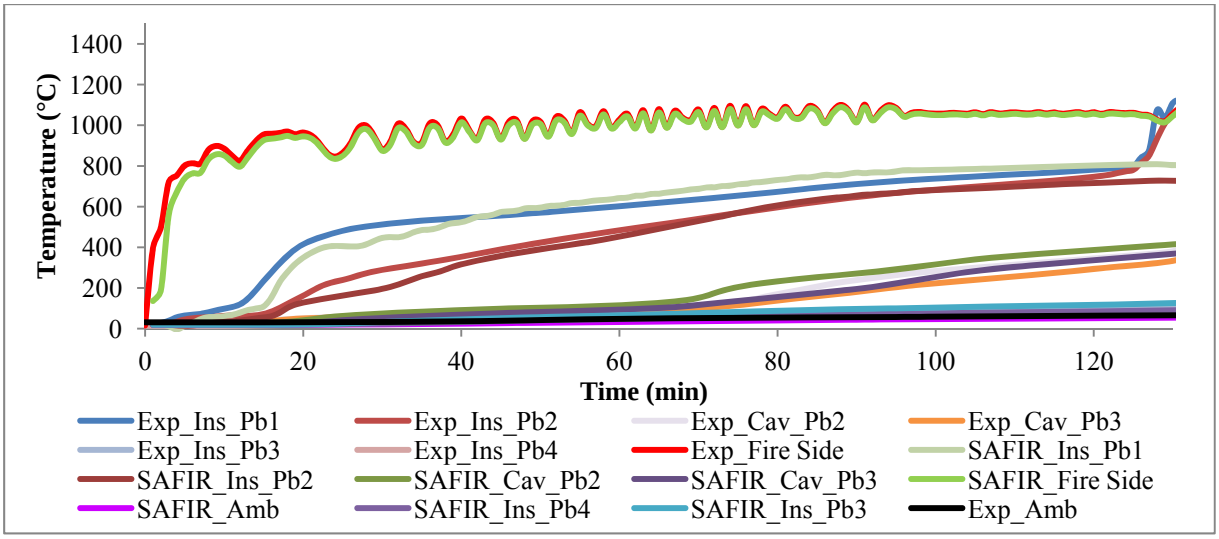

(1) Plasterboard and Insulation

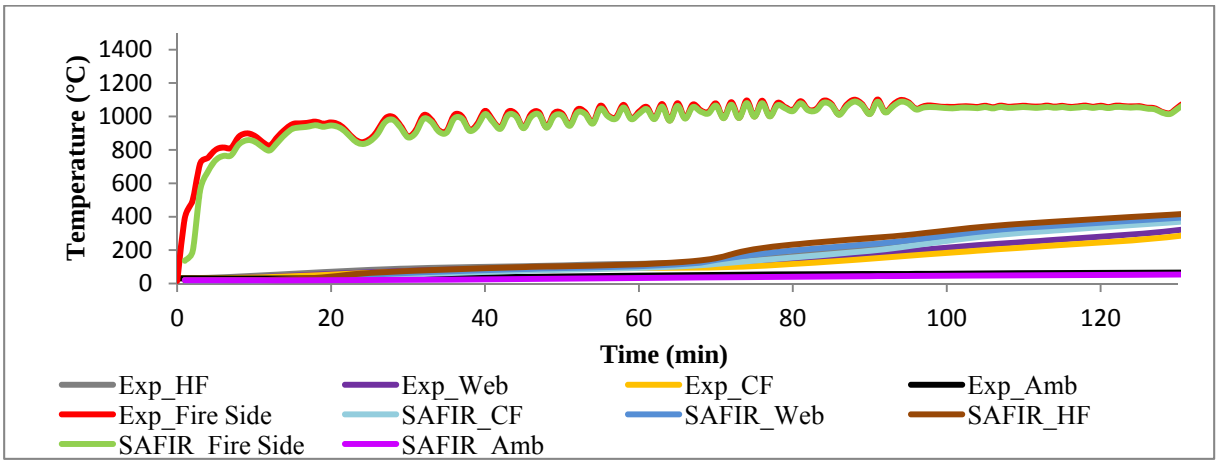

(2) Steel

(h) Test Specimen 9 (cellulose fibre external insulation)

Figure 11: Time-Temperature Profiles of Test Specimens

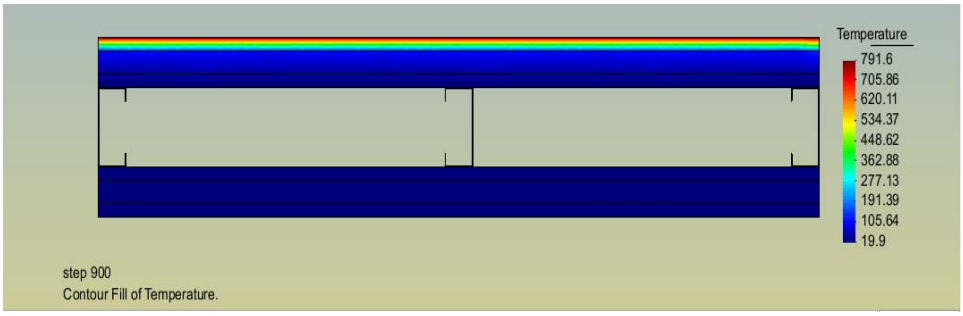

(a) 15 minutes

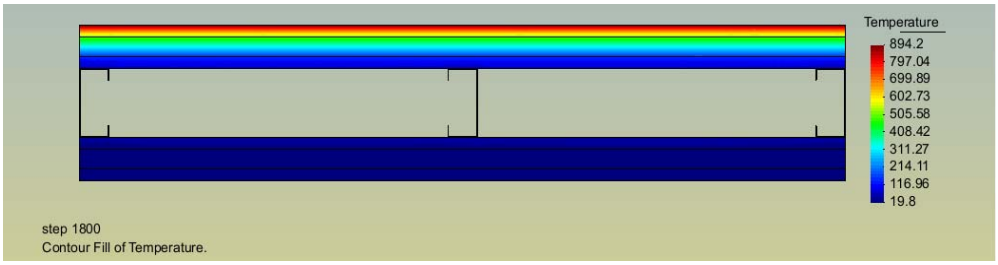

(b) 30 minutes

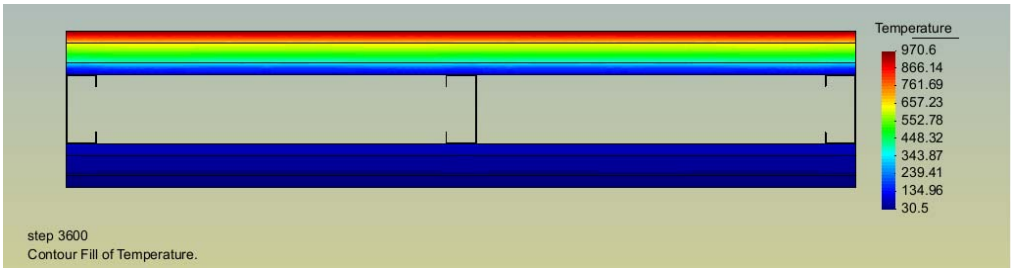

(c) 60 minutes

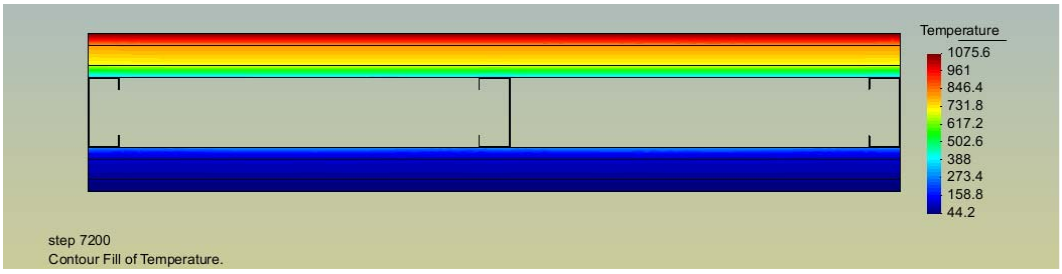

(d) 120 minutes

Figure 12: Temperature Distributions of Specimen 8 under Standard Fire Conditions

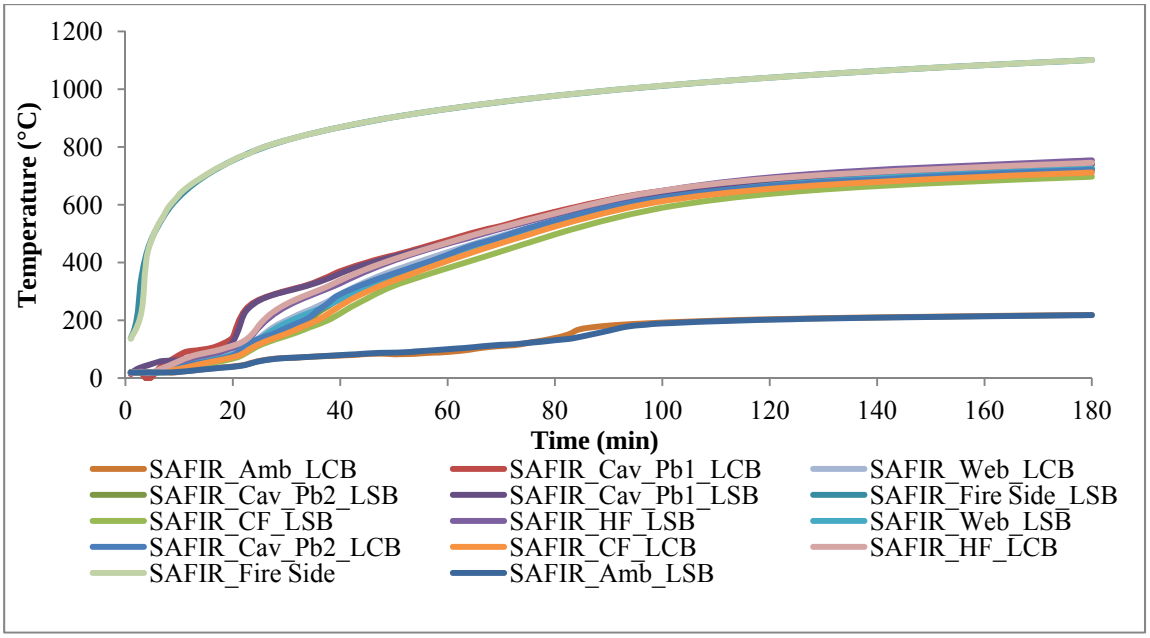

Figure 13: Effect of Stud Section Geometry on the Thermal Performance

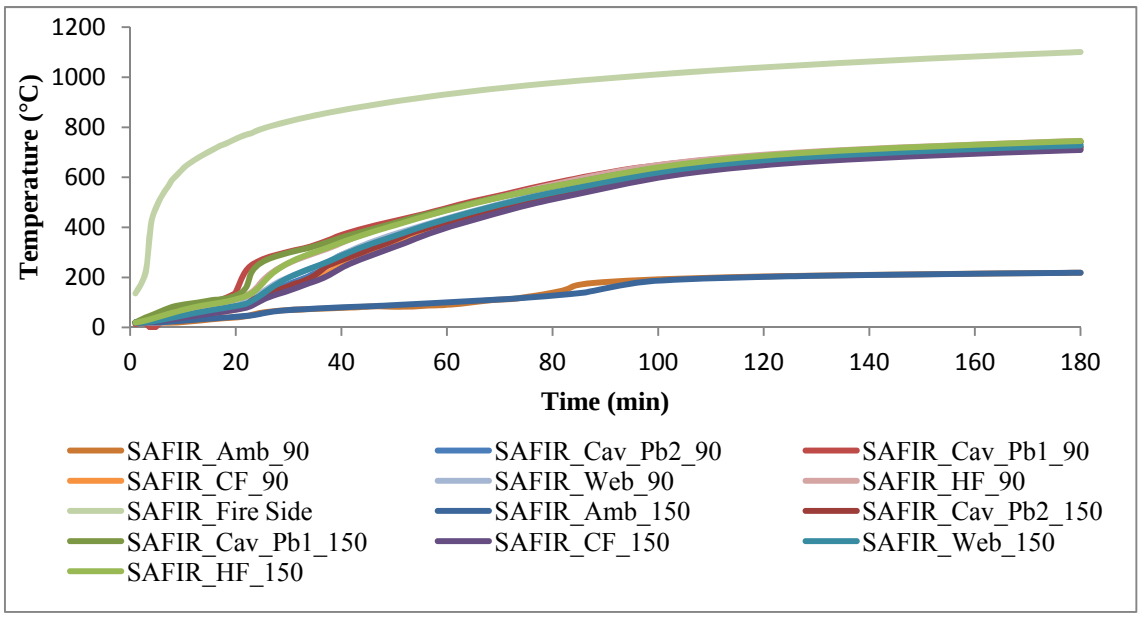

Figure 14: Time-Temperature Profiles of LSF Wall Panels Made of 150x40x15x1.15 LCB and 90x40x15x1.15 LCB

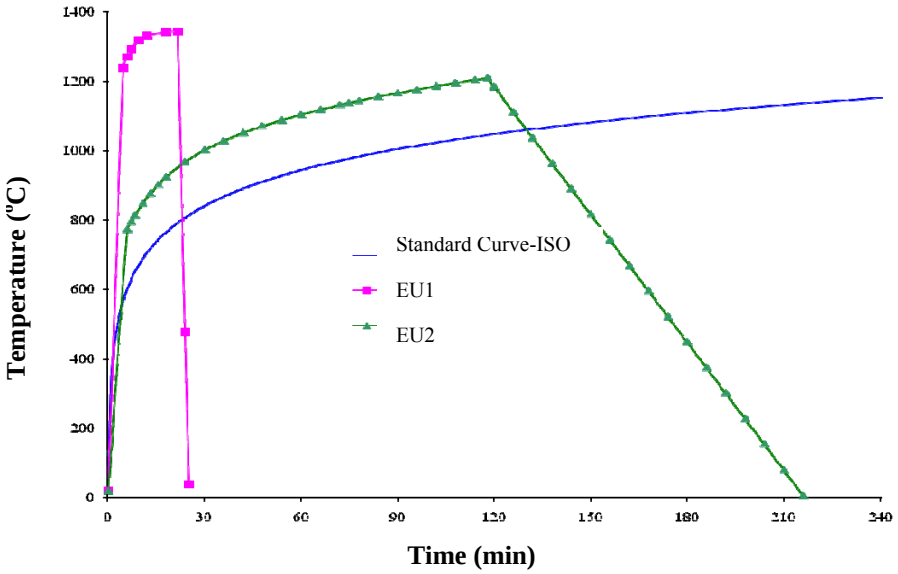

Figure 15: Real Building Curves for Dwellings [24]

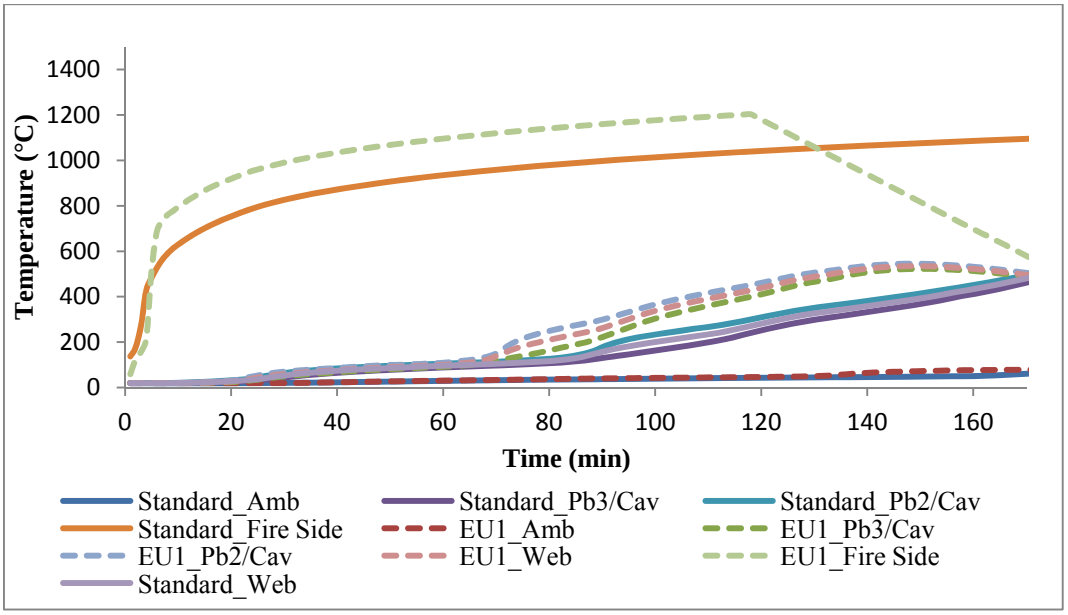

(a) EU1

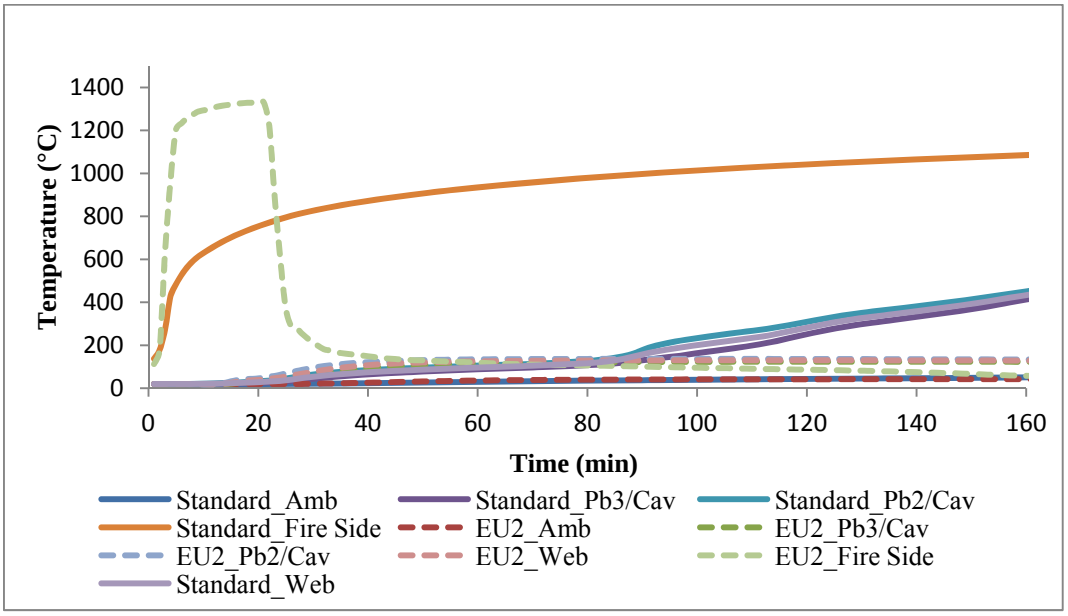

(b) EU2

Figure 16: Time-Temperature Profile of Test Specimen 8 under Real Fire Curves

Table 1: Proposed Specific Heat of Insulations

Insulation Type	Specific Heat (J/(kg°C)
Rockwool	840
Glass Fibre	900
Cellulose Fibre	1250

Table 2: Failure Time of Test Specimens [5]

Test Specimen	Description	Failure Time (min)	Failure Type
1	Single 16mm Plasterboard	89	Insulation
2	Single 16 mm Plasterboard with Vertical Joint	92	Insulation
3	Two 16 mm Plasterboards	180	Pb2 Collapse
4	Two 16 mm Plasterboard with Glass Fibre Cavity Insulation	125	Stud Collapse
5	Two 16 mm Plasterboard with Rockwool Cavity Insulation	145	Stud Collapse
6	Two 16 mm Plasterboard with Cellulose Fibre Cavity Insulation	145	Stud Collapse
7	Two 16 mm Plasterboard with Glass Fibre External Insulation	198	Pb2 Collapse
8	Two 16 mm Plasterboard with Rockwool External Insulation	200	Pb2 Collapse
9	Two 16 mm Plasterboard with Cellulose Fibre External Insulation	163	Pb2 Collapse

List of Figures

List of Tables

Author Biographies

Dr Poologanathan Keerthan is a post-doctoral research fellow in cold-formed steel structures at Queensland University of Technology (QUT), Brisbane, Australia. He has a Bachelor of Engineering degree in Civil Engineering (First Class Hons)-2005 and a PhD in Structural Engineering (QUT)-2009. His research projects have been on the elastic buckling and nonlinear ultimate strength behaviour, shear and bending capacities and fire resistance behaviour of cold-formed steel structures.

Professor Mahen Mahendran has been working as an academic and researcher in structural engineering for more than 25 years. He has a Bachelor of Engineering degree in Civil Engineering (First Class Hons)-1980 and a PhD in Structural Engineering (Monash University)-1985. His research projects included thin-walled steel structures, cyclone/storm resistant buildings and their components, fire safety of structures, wind engineering and disaster mitigation. Most of his research projects have been funded by Australian government and industries since 1991 (valued at more than AUD $4 million).